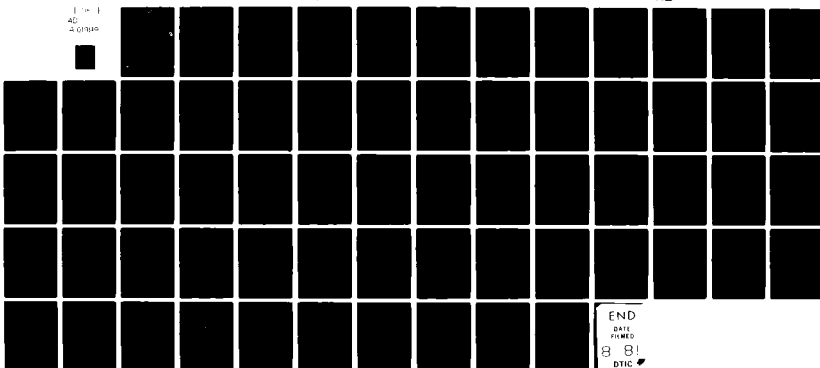


AD-A101 999

MASSACHUSETTS INST OF TECH CAMBRIDGE DEPT OF OCEAN E--ETC F/G 20/11
CRUSHING ANALYSIS OF ROTATIONALLY SYMMETRIC PLASTIC SHELLS. (U)
JUN 81 J G DE OLIVEIRA, T WIERZBICKI N00014-80-C-0616
81-8 NL

UNCLASSIFIED

1 = 1
4D
2 GRIPS



END
DATE
FILED
8-81
DTIC

AD A101999

LEVEL
MASSACHUSETTS INSTITUTE OF TECHNOLOGY
DEPARTMENT OF OCEAN ENGINEERING
CAMBRIDGE, MASS. 02139

12
BS

CRUSHING ANALYSIS OF ROTATIONALLY
SYMMETRIC PLASTIC SHELLS

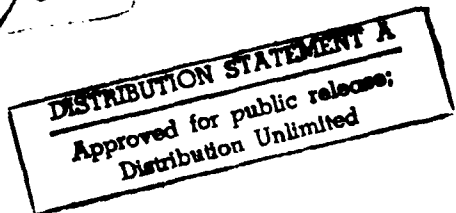
by
Joao G. de Oliveira
and
Tomasz Wierzbicki

Report Number 81-8



- * On leave from the Institute of Fundamental
Technological Research, Warsaw, Poland

30 June 1981
Distribution Unlimited



FILE COPY

146856

81 7 24 020

INDEX

	<u>page</u>
Abstract	ii
1. Introduction	1
2. Analysis of Discontinuities	6
3. Mechanisms of Plastic Deformation	9
4. Determination of the Crushing Force	14
5. Tube Inversion	15
6. Crushing of Conical Shell	17
7. Spherical Shell Under Point Load	19
8. Crushing of a Spherical Shell Between Rigid Plates	25
9. Rigid Boss Loading	27
10. Spherical Cap Under External Pressure Loading	29
11. Effect of End Condition	34
12. Conclusions	35
Acknowledgement	36
References	37
List of Figures	40
Figures	41
Library Card	59
Report Documentation Page	60

Accession For	
NTIS - GRIAL	
DTIC T'B	
Unannounced	
Justification	
By	
Distribution/	
Availability Codes	
Avail and/or	
Dist	Special
A	

Abstract

The crushing analysis of rotationally symmetric plastic shells undergoing very large deflections is presented. A general methodology is developed and simple closed form solutions which can be useful for practical applications are derived for the case of a conical shell and a spherical shell under point load, a spherical shell crushed between rigid plates and under boss loading, and a spherical cap under external uniform pressure. The effect of the end conditions and the limitations of this approach are discussed in detail.

1. Introduction

Thin metal shells of revolution subjected to axisymmetric compressive forces are capable of carrying substantial loads when deflections exceed by one or two orders of magnitude the thickness of the shell, and become comparable to the largest linear dimension of the structure. Thus, the deformation process is far beyond what is commonly understood as post-buckling behavior of elastic or plastic shells. A distinctive feature of such deformation mechanism is that the strain energy function (in the case of elastic shells), or dissipation function (in the case of plastic shells), is concentrated in narrow zones (fold lines or hinge lines) while the remainder of the structure is undergoing a rigid body motion. Furthermore, with some degree of symmetry, the fold lines are forced to move as the deformation process goes on. Depending on the geometrical parameters of the structure and imperfections, either a symmetric or non-symmetric deformation pattern may develop, even though the loading and the structure itself are axially symmetric.

A known example of non-symmetric but regular deflection field is the Yoshimura buckle pattern in compressed thin elastic shells. In the range of very large deflections, the geometry of such a field can be conveniently described using the concept of isometric transformation of surfaces. The foundations of the respective mathematical theory were laid by Pogorielov, [1], who also presented brilliant applications of his theory to the analysis

of post-critical behavior of thin elastic shells, [2]. His work was later followed by Lukasiewicz and Szyszkowski [3], while Foster [4] presented a parallel but independent study of the compression of thin tubes. Pugsley and Macaulay appear to be the first to study the crumpling process of thin cylindrical shells with diamond shape lobes in the plastic range [5]. Although no provision was made to accomodate in the theory the travelling hinges, the corresponding calculations for the mean crushing force, especially the more recent ones [6], agree well with experimental results. Further contribution to the understanding of the process of progressive crumpling of tubes in the multi-lobe modes was made in [7] and [8], but no satisfactory solution of this interesting problem was offered to date.

As tubes get thicker ($R/h < 50$), a well-known transition takes place from the diamond pattern to the crinkling (concertina) mode of deformation, discussed by Alexander [7]. Assuming a simple deformation mechanism with circumferential extension and equating the rate of internal energy dissipation to the rate of work of external forces, he was able to calculate an average crushing force. Minimizing next the force level he evaluated the length of the local buckling wave, and derived a simple expression for the optimal value of the crushing force. The above procedure has proved to be most effective in the approximate analysis of the crumpling process of various thin-walled structures [8,10].

The tube inversion (outside-in or inside-out) is another example of an axially-symmetric deformation of tubes. Two solutions for the magnitude of axial loading necessary to maintain the plastic flow are available. One, due to Al Hassani et al. [10], is good as long as the assumption of a constant thickness holds, and another one, due to Abramowicz [11], takes into account changes of thickness and circumferential curvature. The problem of hemispherical shell or spherical cap loaded by central point-load, rigid boss, or crushed between plates, received much less attention in the literature than the related buckling problem under external pressure loading. Updike and Kalnins performed a thorough analysis of postbuckling behaviour of elastic spherical shells compressed between rigid plates, [12, 13]. Using Reissner equations for shallow rotationally symmetric shells, they determined the force-deflection relationship in subsequent stages of deformation, and the point of bifurcation into a symmetric inward dimple, and later into an unsymmetric shape. In the subsequent study [14] Updike presented an approximate solution for the rigid-plastic shallow shell undergoing symmetric deformations. An extensive theoretical and experimental investigation into this problem was made by Kitching et al. in [15], where the transition into an unsymmetric plastic mode was calculated numerically. Experiments in which polygon rather than circular circumference dimple were observed, were reportedly made earlier by Pian [9].

Leckie and Penny [16] performed a series of tests on carefully manufactured hemispherical shells loaded centrally by a rigid boss. These experiments were followed by a theoretical study due to Morris and Calladine [17], in which the deformed shape of the shell and the force-displacement characteristics were obtained by a sequence of upper bound calculations, in conjunction with an ingeneous idea of treating the shell as a three-dimensional body, [18].

The work of Morris and Calladine constitutes a milestone in the understanding of the crushing behaviour of shells of revolution. It shows through relatively simple numerical calculations that plastic deformations are indeed confined to a relatively narrow ring or section of a toroidal surface, and that the ring is moving outward as the deformation process goes on, leaving a rigid region behind. A snap-through effect was observed whose extent depends on the boss size ρ .

The plastic behaviour of shallow spherical shells under uniform pressure loading is similar to that of a shell under rigid boss loading, as far as the occurrence of the plastic snap-through phenomenon is concerned. This problem was studied by Duszek [19] and Jones and Ich [20], using an approximate yield condition for rotationally symmetric shells. Recently, the same problem was reconsidered by Kondo and Pian [21] by applying the generalized yield line method, which takes into account the changes in the geometry of the structure.

In the present paper we shall extend the approach developed in [7] and [17] to general shells of revolution, with the purpose of deriving some simple results useful for practical purposes. A detailed discussion will be presented on the restrictions imposed on the solution by the conditions of kinematic continuity on the moving hinge circles, and inextensibility of the shell in the meridional direction. Introducing simple displacement and velocity fields, closed-form solutions on the crushing force will be derived for a variety of structures, including conical and hemispherical shells compressed between rigid plates, and a spherical shell under a point-load or central boss loading. The influence of the boss size, and clamped edge conditions will also be discussed at length.

The analysis will be restricted to axisymmetric deformation modes only. A simplified approach to study the lateral crushing of cylindrical shells using a polygon shaped fan of flat elements was developed by Morris and Calladine [22]. This method is particularly suited for treating nonsymmetric but regular deformation modes in hemispherical shells such as the ones observed by Pian [8]. The treatment of non-symmetric problems with smooth deformation fields will be the subject of a future publication [23].

2. Analysis of Discontinuities

The condition of kinematic continuity on the moving hinges or hinge circles in rigid-plastic beams and flat circular plates were formulated by Hopkins [24] and Hopkins and Prager [25]. Before writing the continuity equation for a general shell consider first the one-dimensional case, since the physical arguments leading to these equations are the same.

Let Γ denote a straight line yield hinge whose position on the flat surface element is described by a scalar equation $x = v(t)$. The downward deflection and velocity of the material point lying on the shell middle surface are denoted respectively by $f(x,t)$ and $\dot{f}(x,t)$. We assume that deflections and velocities are continuous at any time and at any point of the shell. Since the deflection f is continuous across Γ , the time derivative of $f(v(t),t)$ along Γ is also continuous across Γ . Thus

$$[f] + \dot{v}(t)[f'] = 0 \quad (1)$$

where the brackets denote discontinuities, if any, of the enclosed quantities across Γ , i.e. $[n] = n_+ - n_-$. Now, \dot{f} is continuous across Γ and Eq. (1) therefore shows that the slope f' can be discontinuous only across stationary yield hinges, for which $\dot{v}(t) = 0$. If the yield hinge Γ is not stationary, then f' must be continuous across Γ . By repeating similar arguments one can show that

$$[f'] + \dot{v}(t)[f''] = 0 \quad (2)$$

provided $\dot{v}(t) \neq 0$.

Consider now a hinge line moving with a constant velocity $\dot{v}(t) = V$ down the undeformed flat surface element leaving a plastically deformed region, Fig. 1. The rate of rotation and curvatures on both sides of the moving hinge are respectively $f_+ = \dot{\theta}$, $f'_- = 0$, $f''_+ = \kappa$, $f''_- = 0$. Now, Eq.(2) reduces to

$$\dot{\theta} + v\kappa = 0 \quad (3)$$

We can see that the moving hinge line imposes a constant curvature $\kappa = \frac{1}{R}$ on the initially flat surface element if the slope of the velocity field $\dot{\theta}$ is related to the hinge velocity by (3).

Return now to the general case, following the derivation presented in [11] and consider a curved discontinuity line Γ moving down the middle surface of the shell χ . The line Γ is dividing the surface χ into two separable parts $\chi = {}^{(+)}\chi \cup {}^{(-)}\chi$. Then ${}^{(+)}\chi$ denotes the deformed part, subjected to plastic deformation. The vector field f is defined over the entire surface χ . Now, the previous analysis still applies except that the first and second derivation of f in (1) and (2) should be replaced by the evaluation of the first and second gradient of f on the surface χ . This is equivalent to the replacement of partial derivatives in (1) and (2) by covariant derivatives, so these equations now read

$$[\dot{f}^i] + v_n [f^i|_\alpha] n^\alpha = 0 \quad i = \{1, 2, 3\} \quad (4)$$

$$[\dot{f}^i|_\alpha] + v_n \left\{ [f^i|_{\beta\gamma}] n^\beta n^\gamma \right\} n_\alpha = 0 \quad \alpha, \beta, \gamma, \delta = \{1, 2\} \quad (5)$$

where n is a surface vector normal to the discontinuity line Γ , while v_n denotes the velocity of the hinge line in the n direction.

Considerable simplification can be obtained in the case of rotationally symmetric shells. The hinge line becomes now a circle and each of the continuity condition (4) and (5) yields only one scalar equation in the meridional plane

$$[f] + v_n [f, \alpha] = 0 \quad (6)$$

$$[\dot{f}, \alpha] + v_n [\dot{f}, \alpha\alpha] = 0 \quad (7)$$

where $[f, \alpha]$ is a jump in the rate of rotation and $[\dot{f}, \alpha\alpha]$ is the corresponding jump in the principle (meridional) curvature.

Take now an intermediate stage of the crushing process where plastic deformations are confined to a relatively narrow zone contained between an inner and outer hinge circle B and C, Fig. 2. The outer hinge circle B moves down the undeformed shell with a velocity v_B imposing a larger curvature, i.e. changing the local radius of curvature from R_B to r_B . The material in front of the hinge is rigid and undergoes a constant and finite rate of rotation $\dot{\omega}$. Thus, the continuity condition reduces in this case to

$$-\dot{\omega}_B + v_B \left(\frac{1}{R_B} - \frac{1}{r_B} \right) = 0 \quad (8)$$

The inner hinge C is travelling with the velocity v_C and removes the curvature, or strickly speaking, it changes the small radius of curvature r_C back to the large one R_C . We can then write

a similar equation to (8) expressing the continuity constraint

$$\dot{\omega}_C + v_C \left(\frac{1}{r_C} - \frac{1}{R_C} \right) = 0 \quad (9)$$

For the material behind the circle C to be rigid, the shell should translate rather than rotate. Hence, there must be at C a counterrotation $\dot{\omega}_C$ of the same magnitude as at B. The condition $\dot{\omega}_B = \dot{\omega}_C$ implies the following relation between the six kinematic and geometric parameters of the problem

$$-v_B \left(\frac{1}{R_B} - \frac{1}{r_B} \right) = v_C \left(\frac{1}{r_C} - \frac{1}{R_C} \right) \quad (10)$$

Equation (10) can be further simplified. If for example the deflected shape of the shell is assumed to be isometric to the original one, it must be its mirror reflection i.e. $R_B \approx R_C$ see [1]. Furthermore the shape of the shell middle surface between the hinge circle B and C may be approximated by a section of a circular toroidal surface so that $r_B = r_C = r$, as suggested in [14,11].

Equation (6) carries the information that the shape of shell at B and C should be continuous at all times, except at the stationary hinge, i.e. at the rigid boss or clamped edge.

In the next section we shall see whether conditions (6) and (10) can be made compatible with other simplifying assumptions regarding the kinematics of the crushing process.

3. Mechanisms of Plastic Deformation

The foregoing analysis has shown that there are two concentrated plastic hinges at B and C and that the cross section

between them rotates as a rigid shape with an angular velocity ω , as the displacement of the shell increases. Our aim is to evaluate the internal energy dissipated in such a mode of deformation. Equating this energy to the rate of work of external forces an instantaneous crushing force can be found necessary to maintain the plastic flow.

The dissipation is due to a discontinuous velocity field at plastic hinges, and to a continuous deformation field in the shell section between B and C. Consider first the latter.

In rotationally symmetric shells there are four components of the generalized strain rate and stress fields. The meridional curvature rate κ_ϕ is infinite at hinge circles and vanishes between them. This follows from the assumption that the rate of rotation is a step function.

It should be noted that the meridional curvature itself κ_ϕ , governed by (8) is kept constant at any material point passing through the plastically deforming annulus, but does not have to be constant along spatial coordinate between B and C.

The circumferential curvature rate κ_θ is continuously changing between B and C from positive $\frac{1}{R_B}$ through zero to negative $\frac{1}{R_C}$, and consequently some energy is dissipated in this deformation mechanism. An exact formula for κ_θ was derived in [11] using a rigorous Eulerian description. In the same paper it was shown that the associated energy dissipation is a small fraction of the total energy.

For the sake of simplicity we shall disregard κ_θ in the equation for the energy dissipation. A very good estimate of the contribution of κ_θ to that energy can be given in a straightforward manner.

Suppose the circumferential curvature is reversed between B and C from $\frac{1}{R}$ to $-\frac{1}{R}$. The rate of work done is twice the energy required to remove the curvature from $\frac{1}{R}$ to zero. The curvature is removed by rotating two ends of a cut circle through the angle 2π , (cf. [26]). Thus, the rate of energy in the considered mechanism of deformation can be approximated by:

$$E(\kappa_\theta) = 2(2\pi) M_0 V = 4\pi M_0 \frac{b}{2} \dot{\omega} \quad (11)$$

where it was assumed that there are no interaction between the circumferential bending moment and the remaining non-vanishing components of the generalized stress field. The velocity V in (11) is an average downward velocity of the deforming zone, $V = \frac{b}{2} \dot{\omega}$; see Fig. 3.

At certain stages of the crushing process considerable meridional membrane forces may be developed. In the present paper the meridional extension rate is assumed to vanish in the zone of continuous deformations. Any extension or shortening of the arc length in the meridional direction is accommodated by the hinge circle B and C. Thus, we do not require inextensibility of the material in the meridional direction but instead extensional plastic hinges are introduced. This assumption is in the spirit of Calladine's approximation in the problem of moderately large deflection of clamped circular plates [18].

The only significant component of the generalized strain rate is the circumferential compression $\dot{\lambda}_\theta$. In order to calculate the associate dissipation energy we shall strictly follow the approach developed in [17], and treat the shell section between B and C as a three-dimensional body. The rate of internal energy dissipation is equal to

$$\dot{E} = \int_V \sigma_0 \dot{\epsilon}_\theta dV = 2\pi \int_S \sigma_0 x \dot{\epsilon}_\theta ds \quad (12)$$

where V and S denote respectively the total volume and area of the cross section between B and C, and x denotes a current distance of the given point F from the axis of symmetry of the shell, see Fig. 3. Note, that the yield stress is positive in tension zones and negative in compression zones. The circumferential strain rate is given by $\dot{\epsilon}_\theta = \frac{\dot{\omega}x}{x}$, where y is the current distance from the axis of instantaneous rotation I-I. The position of this axis with respect to the shell cross section is yet to be determined. Substituting $\dot{\epsilon}_\theta$ in (12) yields

$$E_{int} = 2\pi \sigma_0 \dot{\omega} \int_S |y| ds \quad (13)$$

One has to distinguish now two special cases. If the rise of the toroidal surface over the points B and C is comparable to the shell thickness, the assumption about non-uniform distribution of $\dot{\epsilon}_\theta$ across the thickness is justified, and (13) holds. If the converse is true, one can replace $ds = hdx$, and (13) simplifies:

$$\dot{F}_{int} = 2\pi\sigma_0 h \omega \int_{BC} |y| dx \quad (14)$$

The integral appearing in (14) is the area between the middle surface of the annular section of the shell and the axis of instantaneous rotation, as noted in [14].

The energy dissipated in any of the two plastic hinges is

$$\dot{E}_{int}^{disc} = 2\pi a \int_{-\frac{h}{2}}^{\frac{h}{2}} \sigma_0 \dot{u}_\theta dy = 2\pi a \omega \sigma_0 \int_{-\frac{h}{2}}^{\frac{h}{2}} |y| dy \quad (15)$$

where a denotes the position of the hinge with respect to the axis of symmetry, and \dot{u}_θ is in-plane component of the velocity field. One can easily evaluate (15) as a function of the position of the center of instantaneous rotation with respect to the middle surface of the hinge ξ :

$$\left. \begin{array}{l} \frac{h^2}{4} \\ \xi^2 + \frac{h^2}{4} \\ \xi h \end{array} \right\} \quad \text{for } \xi = 0 \quad (16a)$$

$$\dot{E}_{int}^{disc} = 2\pi \omega \sigma_0 \left. \begin{array}{l} \xi^2 + \frac{h^2}{4} \\ \xi h \end{array} \right\} \quad 0 < \xi < \frac{h}{2} \quad (16b)$$

$$\left. \begin{array}{l} \xi h \end{array} \right\} \quad \text{for } \xi > \frac{h}{2} \quad (16c)$$

In the present approach the hinge circle is indeed a generalized plastic hinge analysed for example by Jones [27], since either bending or extension or both can be developed in it.

The total dissipated energy is the sum of energies dissipated in continuous and discontinuous dissipation fields.

4. Determination of the Crushing Force

In the actual solution the rate of change of external work is always equal to the internal dissipation energy. A similar equality for any kinematically admissible velocity and displacement field can be understood as a definition of the approximate value of the external loading. The more close the assumed fields are to the real one, the better the approximate solution is. A considerable success of this method in predicting the crush behavior of various thin-walled structures (see [7,15]) is due to the correct choice of the admissible field with few free parameters, and also to a somehow weak dependence of the solution on the details of the assumed shape of the shell. For example, any shape of the shell middle surface between inner and outer hinge circles, satisfying kinematic continuity and giving the same area in (14), would yield the same force level. In the present paper we shall take the shape of the shell middle section in the form of a circular or parabolic arc. Furthermore, we shall assume the deformed but rigid portion CD to be a shifted mirror reflection of the original shape AB (dotted line on Fig. 2) by a magnitude b . This implies opposite but equal in magnitude radius of curvature and slopes at points B and C. From the continuity of displacements and slopes at B and C, it follows that the transition shape is determined to within a single parameter which is either the distance between points B and C, or local radius of curvature r . Another free parameter is the position of the axis of rotation ξ .

The rate of work of external loading is

$$P \frac{b}{2} \dot{\omega} - \text{for crushing between plates} \quad (17a)$$

$$P b \dot{\omega} - \text{for point load or boss loading} \quad (17b)$$

Now for any given value of the parameter describing the crushing distance (for example central deflection or central radius of the annular zone), the integral (14) is evaluated and the value of the force P becomes a function of two free parameters ξ and b .

The function $P(b, \xi)$ was studied and it was found that for a certain value of b , the force attains a minimum. On the other hand, except at a very early stage of the crushing process, P attains a lower limit rather than a minimum with respect to $\xi = 0$, Fig. 5.

Assuming the minimum principle to hold for geometrically nonlinear problems, the lowest possible value of P is identified as the best approximate solution. This approach is equivalent to the sequence of upper bound numerical calculations performed by Morris and Calladine [17].

5. Tube Inversion

The approximate solution of the stationary plastic process of tube inversion with various degrees of approximation can be found in [11] and [15]. We shall study the same problem to explain the details of the derivation and to determine the accuracy of the present approach by comparing it with known results.

Consider a tube of the initial radius R being inverted inside out to a final radius $R + 2r$. At the hinge circle B the straight line generator of the cylinder is bent into the curvature $\frac{1}{r}$ and at the hinge circle C the curvature is removed, Fig. 6. A simple and yet accurate solution of this problem, accounting for continuous circumferential extension and concentrated bending at B and C, was worked out by Kitching et al. [15] and has the form

$$\frac{P_{\min}}{2\pi M_0} = 4 \sqrt{\frac{3r}{h}} \approx 6.92 \sqrt{\frac{R}{h}}, \quad r = \sqrt{\frac{Rh}{3}} \quad (18)$$

In order to apply the present approach, we assume that the portion of the shell between hinge circles B and C form one half of the toroidal surface. We also assume for simplicity that $r/h > 1$, so that Eq. (14) applies and $\xi = 0$. The distance between B and C is $h = 2r$ and the integral appearing in (16) represents the area of the half circle. Using this result and Eq. (15), the rate of energy balance equation yields

$$Pr \dot{\omega} = 2\pi \sigma_0 h \omega \frac{\pi r^2}{2} + 2\pi \sigma_0 \omega \frac{h^2}{4} [R + (R+2r)] \quad (19)$$

The rate of infinitesimal rotation $\dot{\omega}$ drops out from both sides of (19) and the dimensionless force becomes

$$\frac{P}{2\pi M_0} = 2 \left[\frac{\pi r}{h} + \frac{R}{r} + \frac{1}{3} \right] \quad (20)$$

Minimizing the right hand side of (20) with respect to r and substituting the optimal radius back into (20) we can obtain the final formula:

$$\frac{P_{\min}}{2\pi M_O} = 4 \sqrt{\frac{\pi R}{h}} + 2 \approx 7.09 \sqrt{\frac{R}{h}} + 2; r = \sqrt{\frac{Rh}{\pi}} \quad (21)$$

The above results compares well with solution (18), especially for large R/h.

It is interesting to estimate the effect of the variable circumferential curvature, according to the approximate formula (11). One can easily find that the magnitude of the non-dimensional force in (21) increases then by 2, which again is a small contribution for large R/h. At the same time the optimum radius of inversion remains the same.

It can be checked that the condition (10) of kinematic continuity, reduces now to $\frac{V_B}{r} = \frac{V_C}{r}$ and thus is satisfied.

Finally it should be noted that the crushing force of a tube loaded by a central force rather than crushed between plates, is one half of that predicted by (21).

6. Crushing of a conical shell

The geometry of the partially crushed conical shell is shown in Fig. 7. We assume that the portion of the shell subjected to localized plastic deformation forms a section of a toroidal surface and that the inverted cone is of the same angle α . The area of the section of a circle between the points E and C is $S = \frac{r^2}{2} [(\pi - 2\alpha) - \sin(\pi - 2\alpha)]$ and the distance $b = 2rc\cos\alpha$. It is now straightforward to work out the solution which takes the form

$$\frac{P_{\min}}{2\pi M_O} = \frac{4}{\cos\alpha} \sqrt{\frac{a}{h}} \sqrt{(\pi - 2\alpha) - \sin(\pi - 2\alpha)} \quad (22)$$

$$r = \sqrt{\frac{ha}{(\pi - 2\alpha) - \sin(\pi - 2\alpha)}} \quad (23)$$

Here a is the measure of the crushing distance, which is related to the central deflection by

$$w = \frac{2a}{\tan\alpha} \quad (24)$$

The formulas become increasingly inaccurate for $\alpha \rightarrow \frac{\pi}{2}$ and also for small $\frac{a}{h}$, since then the assumptions leading to $\xi = 0$ are not satisfied. In these cases a more exact solution can be obtained when needed, using (13) rather than (14) and minimizing the solution with respect to ξ .

Equation (23) predicts an increasing radius of the toroidal surface, $r > 0$, as the crushing zone is expanding. The change of the radius is related to velocities of hinge circles by

$$2\dot{r} = (V_B - V_C) \tan\alpha \quad (25)$$

At the same time we have assumed that $R_B = R_C = \infty$ and $r_B = r_C$ which yields $V_B = V_C$. We see that the condition of kinematic continuity is not satisfied by the present solution. The difficulty encountered can be overcome by considering the general case in which $r_B \neq r_C$ $R_C \neq \infty$. Now, the toroidal surface ceases to be of a circular cross-section and the hinge circles B and C will no longer be positioned on the same level. As a result membrane force will develop in the hinge C which would result in a slight increase of the force level. Also, with a variable radius $R_C(a)$ the hinge circle will produce a curved line rather than a conical one on the meridional plane. It is not difficult to write

a system of ordinary differential equations with a shifted argument describing variation of v_B v_C r_B r_C and R_C with the crush distance. We shall not attempt to study this system since it is believed that insignificant changes would have then been introduced to the solution. The problem however is interesting by its own right.

7. Spherical Shell Under Point Load

This problem has been analysed in [27] but as we shall see, its range of validity is very small. Morris and Calladine [17] evaluated the force-deflection relationship for a particular shell with $R/h = 60$ up to a deflection ratio $w/h = 6$.

Let the current position of the outer hinge circle on the shell be defined by the angle α , see Fig. 8. The distance between the two hinge lines b is related to the radius of the toroidal surface through $b = 2rs\sin\alpha$. The expression for the crushing force, derived in an analogous way as in the case of a conical shell, has the form

$$\frac{P_{\min}}{2\pi M_O} = 2 \sqrt{\frac{R}{h}} - 1 \quad (26)$$

$$r^2 = \frac{hR}{n} \quad (27)$$

$$\text{where } n = \frac{2\alpha - \sin 2\alpha}{\sin \alpha} \quad (28)$$

From purely geometrical considerations we can derive a relation between the angle α and the crush distance w

$$\frac{w}{h} = 2 \frac{R}{h} (1 - \cos \alpha) - \frac{R}{h} \left[1 - \sqrt{1 - 4 \frac{h}{R} \frac{\sin^2 \alpha}{n}} \right] \quad (29)$$

Equations (26) and (29) furnish a parametric representation of the function force versus displacement. A plot of this function for several values of the radius to thickness ration R/h is shown in Fig. 9. The dependence of the solution on R/h appears to be weak. Indeed, treating $\frac{h}{R}$ as a small parameter and expanding the square root in (29) in power series with respect to $\frac{h}{R}$ around $\frac{h}{R} = 0$ one gets

$$\sqrt{1 - 4\frac{h}{R} \frac{\sin^2 \alpha}{n}} = 1 - 2 \frac{\sin^2 \alpha}{n} \frac{h}{R} + \dots \quad (30)$$

so that (29) can now be approximated by

$$\frac{w}{h} = 2 \frac{R}{h} (1 - \cos \alpha) - 2 \frac{\sin^2 \alpha}{n} \quad (31)$$

Combining next (26) and (31) to eliminate the parameter R/h we obtain

$$\frac{w}{h} = \left(\frac{P_{\min}}{2M_0 \pi} + 1 \right)^2 \left\{ \frac{1 - \cos \alpha}{2n(\alpha)} \right\} - 2 \left\{ \frac{\sin^2 \alpha}{n(\alpha)} \right\} \quad (32)$$

Expanding the trigonometric function appearing in (32) in power series and retaining terms up to the third power, the two coefficients in (32) become

$$\frac{1 - \cos \alpha}{2n(\alpha)} = \frac{1}{4} \cdot \frac{2\sin \alpha - \sin 2\alpha}{2\alpha - \sin 2\alpha} \approx \frac{3}{16} \quad (33a)$$

$$\frac{2\sin^2 \alpha}{n} = \frac{2\sin^3 \alpha}{2\alpha - \sin 2\alpha} \approx \frac{3}{2} \left(1 - \frac{\alpha^2}{6} \right) \quad (33b)$$

Thus, the first coefficient turns to be constant, while the second varies very little which α , especially for $\alpha < 1$. Substituting (33) back into (32), the final formula for the force-deflection relationship takes the form

$$\frac{w}{h} = \frac{3}{16} \left(\frac{P_{\min}}{2\pi M_O} + 1 \right)^2 - \frac{3}{2} \quad (34)$$

The plot of the function (34) is given in Fig. 9 by a broken line. The agreement with the exact solution (full line), which depends on R/h , is seen to be very good.

It is interesting enough that the same solution can be obtained by making a different set of assumptions. Suppose the hemispherical shell is approximated by a parabolical shell. The relationship between the angle α and central deflection is now given by

$$\frac{w}{h} = \frac{R}{h} \sin^2 \alpha - \frac{b^2}{2hR} \quad (35)$$

Replacing likewise the circular cross-section of the toroidal surface by a parabolic arc

$$y = \frac{\left(\frac{b}{2}\right)^2 - x^2}{2r} \quad (36)$$

the area integral in (14) can be readily evaluated, and the expression for the crushing force takes the form:

$$\frac{P}{2\pi M_O} = \frac{2}{3} \frac{b}{h} \sin \alpha + \frac{2R \sin \alpha}{b} - 1 \quad (37)$$

Optimization the right hand side of (37) with respect to b results in

$$b^2 = 3hR \quad (38)$$

Now combining (35), (37) and (38), the expression (34) for the crushing force is obtained in the same form as before. This result is important from the practical point of view, since the mathematics

involved in the alternative derivation of (34) are much simpler. We shall take advantage of this property, and in the remainder of the paper dealing with spherical shells always replace a circle by a parabolic arc. Note that by doing so the condition of continuity of slope of the displacement field (6) is not satisfied, but as we have seen, the solution is hardly affected by this.

The second continuity condition (10) reduces now to

$$\frac{v_B}{v_C} = \frac{1 - \frac{r}{R}}{1 + \frac{r}{R}} \quad (39)$$

which means that $|v_B| \neq |v_C|$. On the other hand formula (38) in the present solution implied that $b \neq 0$. Recalling that $b = (v_B - v_C) \cos\alpha$, we have $|v_B| = |v_C|$, which contradicts the condition of continuity. A consistent set of equations can be written, as discussed previously. However, the resulting solution, which apparently loses its appealing simplicity, is believed to introduce insignificant changes and thus will not be discussed further.

The present solution with two moving hinges becomes increasingly inaccurate with decreasing value of the parameter α . Two factors are responsible for that. First, at an early stage of the crushing process, only one hinge circle is formed and the kinematics of the process does not involve a free parameter to be optimized. Secondly, for small α the portion of the toroidal shell becomes relatively shallow so that the assumption leading to $\xi = 0$ is no longer valid, and the shell should be treated as a three-dimensional body, according to the method developed by

Calladine [18]. We shall study these two cases separately.

Assume that the radius of the inner hinge is zero. From simple geometrical consideration Fig. 10, it follows that

$$b = R \sin \alpha, \quad R = 2r \quad (40)$$

Introducing (40) into (35) and (37) and eliminating k/h we obtain the following force-deflection characteristics

$$\frac{P}{2\pi M_0} = \frac{4}{3} \frac{w}{h} + 1 \quad (41)$$

which is identical to the one derived in [27]. The function (41) represents a straight line intersecting the curve described by (34) at $\frac{w}{h} = \frac{3}{2}$, Fig. 11.

Return now to the general case of the shell in which the internal energy dissipation is governed by (13) and (16b). We assume that (40) holds, and that the shape of the shell middle surface represents a parabolic arc. The energy balance equation can be written in the form

$$Pb = 2\pi\sigma_0 \cdot 2 \int_0^{\frac{b}{2}} \left\{ \int_0^{y^I} y dy + \int_0^{y^{II}} y dy \right\} dx + \left(\frac{h^2 b}{4} + \xi^2 b \right) 2\pi\sigma_0 \quad (42)$$

where y^I and y^{II} are respectively the upper and lower contour of the shell cross-section, measured from the axis of instantaneous rotation, see Fig. 4.

$$y^I = \frac{\left(\frac{b}{2}\right)^2 - x^2}{R} + \frac{h}{2} - \xi \quad (43a)$$

$$y^{II} = - \frac{\left(\frac{b}{2}\right)^2 - x^2}{R} + \frac{h}{2} + \xi \quad (43b)$$

The integrals in (42) can be readily evaluated and the crushing force becomes a function of a single parameter ξ

$$\frac{P}{2\pi M_o} = 2 + 8\left(\frac{\xi}{h}\right)^2 - \frac{4}{3}\left(\frac{\xi}{h}\right)\frac{b^2}{Rh} + \frac{8}{15}\frac{b^4}{R^2 h^2} \quad (44)$$

Introduction (40) into (35) we obtain a unique relation between the radius of the hinge and central deflection

$$\frac{w}{h} = \frac{b^2}{2hR} \quad (45)$$

The minimization of the right hand side of (44) yields an optimum value of the parameter ξ

$$\frac{\xi}{h} = \frac{1}{12} \frac{b^2}{Rh} = \frac{1}{6} \frac{w}{h} \quad (46)$$

Substituting (45) and (46) back into (44) we finally obtain

$$\frac{P}{2\pi M_o} = 2 + \frac{14}{45} \left(\frac{w}{h}\right)^2 \quad (47)$$

The above relation is depicted in Fig. 11 by a solid line.

Equation (47) is valid as long as the line of instantaneous rotation first touches either the inner or outer contour y^I or y^{II} . This first occurs at $\frac{w}{h} = \frac{3}{2}$. Thus, the range of applicability of both solutions appears to be the same. The formula (41) is easy to evaluate but it gives unsatisfactory results for $w/h = 0$. This will become even more evident in the problem of a shell loaded by a rigid boss. On the other hand, the solution (47) predicts correctly the yield point load but the mathematics involved are much more complicated.

The 4% difference between the functions (34) and (47) at $w/h = \frac{3}{2}$ is attributed to the fact that the former involves the simplifying assumption $\xi = 0$, while the latter not. By continuing the exact calculation beyond that point, the corresponding solution (dotted line in Fig. 11) would gradually converge to the curve representing the formula (34). The thin full line in the same figure denotes the Morris and Calladine numerical solution. Unfortunately, no information was given in [17] on the magnitude of the integration step employed so it is difficult to assess its accuracy. A good agreement of both solutions is observed over the entire range of deflection covered by the Morris and Calladine solution.

8. Crushing of a Spherical Shell Between Rigid Plates

The procedure for solving this problem essentially follows that presented in the preceding section, except that now the rate of external work should be computed according to (17b) and the relation between w and α is different. As before,

the analysis follows several stages. The yield point and post-yield behavior is accurately predicted by the formula

$$\frac{P}{2\pi M_o} = 4 + \frac{5}{2} \left(\frac{w}{h}\right)^2 \quad (48)$$

valid for $\frac{w}{h} \leq \frac{3}{2}$. In the later stage of the crushing process, when the inner hinge leaves the shell axis, the plate displacement is related to the angle α by

$$\frac{w}{h} = \frac{R}{2h} \sin^2 \alpha - \frac{h}{4h} \sin \alpha \quad (49)$$

The optimum value of width of the deforming radius is the same as before $b = \sqrt{3hR}$, Equation (38), and the resulting force-deflection relationship takes the form

$$\frac{w}{h} = \frac{1}{43} \left(\frac{P}{2\pi M_o} + 2 \right)^2 - \frac{3}{32} \left(\frac{P}{2\pi M_o} + 2 \right) \quad (50)$$

The above solution is valid theoretically until the crush distance reaches the shell radius $w = R$. It is interesting to compare the formula (50) with an approximate solution due to Updike [14]:

$$\frac{w}{h} = \frac{1}{48} \left(\frac{P}{2\pi M_o} \right)^2 \quad (51)$$

which was believed by the author to be valid for deflections not exceeding about one tenth of the shell radius. When both solutions are plotted, it is seen that a relative difference between them is small over the entire range of variation of w , Fig. 12.

9. Rigid Boss Loading

Leckie and Penny performed a series of tests on carefully manufactured spherical shells with $R/h = 60$ and variable boss size [16]. They observed that with increasing downward deflection the crushing force for a given radius of the boss ρ reaches a maximum, then drops suddenly as the shell buckles, and starts to rise again. They also found that the initial plastic yield-point load depends markedly on a single geometrical parameter

$$\beta = \frac{\rho}{\sqrt{Rh}} \quad (52)$$

but with increasing deflection this dependence is much less pronounced. However, the tests were not run far enough to decide whether all $P - w$ curves did converge to a single one.

Assuming a rigid perfectly plastic material idealization Morris and Calladine [17] were able to predict accurately the initial response of the shell. Their numerical calculations have shown that while the slope of the load-deflection curves becomes the same for $\frac{w}{h} \geq 2$, the curves corresponding to different β are considerably shifted with respect to one another.

It is reasonable to expect that the effect of the boss size is a local one and should be almost entirely "forgotten" by the shell at later stages of the deformation process, so that all curves would eventually converge. Indeed, the deformation mechanism with expanding ring of plastic deformation is the same as before, except that the reference point for measuring deflection changes with the boss size. This gives rise to a new term

in the force-displacement relationship

$$\frac{w}{h} = \frac{3}{16} \left(\frac{P}{2\pi M_0} + 1 \right)^2 - \frac{3}{2} - \frac{\beta^2}{2} \quad (53)$$

The above solution reduces to the one describing the shell under central-point load (formula (34)) by setting $\beta = 0$. The new term is relatively small, and provides a shift of $P - w$ curves in the w/h direction Fig. 13. The horizontal displacement of $P-w$ curves in the numerical solution reported in [17] for the same values of β are much larger, which is probably attributed to the trial and error optimization procedure employed.

We were unable to derive a simple closed-form solution for the initial phase of loading based on the exact formula (13) showing the nature of the convergence. However, the interesting pattern of behavior of the shell associated with plastic snap-through can be described, at least qualitatively using the approximate formula (14). Assuming that a stationary hinge circle is formed at $\Gamma = \rho$ and the moving one at $\Gamma = \rho + b$, the load-deflection relationship was found to be

$$\frac{P}{2\pi M} = \frac{2}{3} \left[\sqrt{2 \frac{w}{h} + \beta^2} - \beta \right] \sqrt{2 \frac{w}{h} + \beta^2} + \frac{2\beta}{\sqrt{2 \frac{w}{h} + \beta^2} - \beta} + 1 \quad (54)$$

The above solution reduces to (41) for $\beta = 0$ but it leads to an unrealistic infinite force magnitude with $\frac{w}{h} \rightarrow 0$. This is a consequence of the assumed symmetric geometrical shape of the shell cross-section (36) with zero initial width of the plastic zone to initiate the motion. In reality, the shape is unsymmetric with finite width. It was possible to derive an approximate expression for the initial yield-point load ($w/h = 0$) in the form:

$$\frac{P}{2\pi M_0} = 8\beta, \quad b = \frac{\sqrt{Rh}}{2\beta} = \frac{Rh}{2\rho} \quad (55)$$

The plot of the function (54) with (55) for several values of the parameter β is shown in Fig. 14.

10. Spherical Cap Under External Pressure Loading

Consider a simply supported spherical shell with base radius a , and rise H , Fig. 15. The shallowness of the shell is described by the parameter

$$\alpha = \frac{a^2}{2hR} = \frac{H}{h} \quad (56)$$

Following Ref. [21] define the total load P and the reference load P_0 by

$$P = \pi p a^2 \quad P_0 = 6\pi M_0 \quad (57)$$

where p is a uniformly distributed downward pressure. It is relatively easy to derive the load-deflection relationship for any value of α , using the present method. We shall however restrict the analysis to the limiting cases of small and large α . Consider first the case $\alpha \gg 1$ for which equation (14) applies. Suppose the outer boundary of the plastically deforming zone BC is b while the portion AB remains rigid. The assumed velocity field consist, as previously, of the rotation around the point B

$$\dot{w}(x) = \dot{\omega}x \quad (x \leq b \leq a) \quad (58)$$

This rotation imposes a continuous change in the initially circular shape of the shell middle surface. If the central deflection is smaller than the rise of the shell above the circle b , $w < \frac{b^2}{2R}$, the current shape can be approximated by

the parabolic arc.

$$y(x) = \frac{2b^2}{2R} \left(\frac{x}{b}\right) - \left(\frac{b^2}{2R} + w\right) \left(\frac{x}{b}\right)^2 \quad (59)$$

For the time being we assume the plastic hinge circle to be located somewhere between the shell center and the support $0 < b \leq a$. Equating the rate of external work to the energy dissipated in the region of continuous deformation and plastic hinge circle one gets

$$2\pi \int_0^b p\omega(x)xdx = 2\pi\sigma_0 h\omega \int_0^b y(x)dx + 2\pi\sigma_0 \frac{h^2}{4} wb \quad (60)$$

or after integration

$$\frac{P}{P_0} \frac{\bar{b}}{\alpha} = \frac{8}{3} \bar{b} - \frac{4}{3} \frac{w}{h} + 1 \quad (61)$$

where $\bar{b} = \frac{b^2}{2hR}$. We can see that for the force to be a minimum one has to consider the largest possible value of \bar{b} , i.e. $\bar{b} = \alpha$. With the assumed simply supported boundary conditions there will not be any contribution of the concentrated hinge to the total dissipation energy, and the last term in Eq. (61) should vanish, giving the final expression for the force deflection characteristics

$$\frac{P}{P_0} = \frac{8}{3} \alpha - \frac{4}{3} \frac{w}{h} \quad \text{for } w < \alpha \quad (62)$$

In particular, the initial yield-point load is obtained from (62) by putting $w = 0$, $P/P_0 = 8/3\alpha$. A plot of the above formula is undistinguishable from the curve representing the much more complicated solution derived by Kondo and Pian [21], Fig. 16

At the other extreme we have very shallow shells in which the line of instantaneous rotation lies within the contour of the shell cross-section, Fig. 4. This implies $\alpha \leq 1$.

Assume that the shape of the shell middle surface is changing with deflections according to Eq. (59). The energy in the continuous deformation field is given by

$$\dot{E}_{\text{cont.}} = 2\pi\sigma_0 \int_0^b \left\{ \int_0^y y^I dy + \int_0^{y^{II}} y dy \right\} dx \quad (63)$$

where the limits of the integrals appearing in (63) are

$$y^I = y + \frac{h}{2} - \xi \quad (64a)$$

$$y^{II} = -y + \frac{h}{2} + \xi \quad (64b)$$

The expression for the energy dissipated at the outer hinge would depend on the position of the hinge circle. If $b < a$, then the boundary conditions do not have any effect on the solution and Eq. (16b) applies. If the plastic zone extends up to the support, $b = a$, then for a simply supported shell restrained from axial motion, the term responsible for bending vanishes

$$\dot{E}_{\text{hinge}} = 2\pi\sigma_0 \dot{\omega} b \left[n \frac{h^2}{4} + \xi^2 \right], \quad n = \begin{cases} 1 & \text{if } b < a \\ 0 & \text{if } b = a \end{cases} \quad (65)$$

The left hand side of the energy balance equation is the same as before (60), while the right hand side is a sum of (63) and (65). Evaluating the integral, one obtains

$$\frac{P}{P_0} \frac{\bar{b}}{\alpha} = (1 + n) + \frac{32}{15} \bar{b}^2 - \frac{12}{5} \bar{b}\bar{q} + \frac{4}{5} \bar{q}^2 + 2\bar{\xi}^2 - \frac{4}{3} \bar{\xi}(2\bar{b} - \bar{q}) \quad (66)$$

where $\bar{\xi} = \frac{2\xi}{h}$, $\bar{q} = \frac{w}{h}$

After minimization with respect to ξ , the formula (66) becomes

$$\frac{P}{P_0} \frac{\bar{b}}{\alpha} = (1 + \eta) + \frac{56}{45} \bar{b}^2 - \frac{68}{45} \bar{b}q + \frac{26}{45} q^2 \quad (67)$$

The load-deflection curve, represented by (67) is dropping with increasing \bar{b} and attains the lowest position when

$$\bar{b}^2 = (1 + \eta) \frac{45}{56} + \frac{26}{56} q^2 \quad (68)$$

For example at $q = 0$, the optimum value of radius of the outer hinge is $\bar{b} = 1.3$, falling beyond the range of applicability of the present solution, which is $\bar{b} \leq \alpha \leq 1$. Consequently, the least value of the crushing force is obtained by taking the largest possible radius, i.e. $\bar{b} = \alpha$. We have thus shown that for shallow shells the zone of continuous plastic deformations is extending right up to the support. Substituting $\eta = 0$ and $\alpha = \bar{b}$ into (59), leads to the following force-deflection relation.

$$\frac{P}{P_0} = 1 + \frac{56}{45} \alpha^2 - \frac{68}{45} \alpha q + \frac{26}{45} q^2 \quad (69)$$

In particular, the initial yield-point load is given by

$$\frac{P}{P_0} = 1 + \frac{56}{45} \alpha^2 \quad \alpha \leq 1 \quad (70)$$

In deriving Eq. (69), shell deformations both in radial and circumferential directions were taken into account. A relative contribution of the two components of the dissipated energy is controlled by the position of the axis of instantaneous rotation I-I. The optimum position is one which minimizes the magnitude of the pressure required to maintain the plastic flow. It is interesting to note that the neglect of meridional strain, an assumption made in Ref. [21], would lead to an increase rather

than decrease in the level of the yield-point load. Indeed, in the present approach all work done by the meridional strain is concentrated in the generalized tensile hinges and the corresponding dissipation energy is given by (65). This term can easily be made equal to zero by taking $\xi = 0$. Substituting $a = b$ and $\xi = 0$ into (66) we obtain a new solution

$$\frac{P}{P_0} = 1 + \frac{32}{15} \bar{b}^2 - \frac{12}{5} \alpha q + \frac{4}{5} q^2 \quad (71)$$

Load-deflection curves for few chosen values of the parameter α are shown in Fig. 17 together with the solution due to Kondo and Pian. The initial yield-point load is obtained from (71) by setting $q = 0$:

$$\frac{P}{P_0} = 1 + \frac{32}{15} \alpha^2 \quad \alpha \leq 1 \quad (72)$$

The above formula is identical to the one derived by Kondo and Pian and the corresponding $P - \alpha$ curve clearly lies above that given by (70), Fig. 16. Thus, the neglect of meridional strain rate was offset by even larger increase of the dissipation due to the circumferential strain rate. With increasing α , the contribution of dissipated energy in meridional direction diminishes, illustrating a nature of the approximation introduced in replacing (13) by (14). Note that the solution (62) was derived on the assumption that $\xi = 0$, and this explains the excellent correlation of the present solution with the more elaborate solution due to Kondo and Pian, which employs a full set of equations describing moderately large deflection of shells.

It is not in principle difficult to extend the present solution to shells with intermediate values of the parameter α . The $P - \alpha$ curve would first follow Eq. (70) and then converge asymptotically to Eq. (62).

11. Effect of End Condition

According to the present analysis, the boundary conditions are not felt by the shell until the outer hinge reaches the support located at ϕ^* . It is seen from (35) and (38) that this occurs when deflections become

$$\left(\frac{w}{h}\right)^* = \frac{\rho\alpha^2}{Rh} - \frac{3}{2}, \quad \sin\alpha^* = \frac{\rho^*}{R} \quad (73)$$

For a shell under central-point load, the width of the plastic zone predicted by the approximate solution is $b = \sqrt{3Rh}$. From now on the outer hinge remains fixed, and any further increase of w/h is due to the diminishing of the width of the toroidal section b . Introducing the dimensionless parameter $\alpha = \frac{b}{\sqrt{3Rh}}$, the geometrical relation becomes

$$\frac{w}{h} = \frac{\rho^*}{hR} - \frac{3}{2}\alpha^2 = \frac{w^*}{h} + \frac{3}{2}(1 - \alpha^2) \quad (74)$$

For fully clamped boundary conditions, the solution (37) with two concentrated plastic hinges still applies, so that after introducing (73) into (37) we have

$$\frac{P}{2\pi M_O} = 2 \frac{\rho^*}{\sqrt{3Rh}} \left(\alpha + \frac{1}{\alpha} \right) - 1 \quad (75)$$

Equations (74) and (75) provide a parametric representation of the load-deflection relationship at the terminal stage of the shell motion

With $\alpha \rightarrow 0$ the force blows up to infinity. Fig. 18. This occurs when $\frac{w}{h} = \frac{w^{**}}{h} = \frac{w^*}{h} + \frac{3}{2}$. In reality the force level in shells subjected to central point load is equal to the strength of the inverted spherical shell in tension. An upper bound for this force is

$$\frac{P_{\text{tens}}}{2 M_0 \pi} = \frac{4R}{h} \quad (76)$$

This is much higher than (75) with $\alpha = 1$, but finite. For shells compressed between rigid plates the formula (75) applies multiplied by the coefficient 2. The force increases with α approaching zero and indeed goes to infinity when the upper plate comes in contact with the supporting plate. A typical loading situation for the two cases described above is shown in Fig. 18.

12. Conclusions

This paper presents a general methodology for predicting the crush resistance of arbitrary rigid plastic shells of revolution deforming in an axisymmetric mode. The implications of the conditions of kinematic continuity, as well as the boundary conditions, are discussed. Several practical problems are solved, including a conical shell and a spherical shell crushed between rigid plates and under boss loading, and a spherical cap under external uniform pressure.

For the initial stage of deformation the structure has been treated as a three dimensional body, in the spirit of Calladine's approach [18], while in subsequent stages a simplification to this approach has been suggested, which results in simple closed form solutions useful for engineering applications. A good correlation

was found with some existing solutions of similar problems obtained through much lengthier calculations.

In all cases treated, the zone of plastic deformation was found to be confined to a relatively narrow region. Also, the level of the crushing force was shown to be quite insensitive to the particular shape of that zone.

The present method makes it possible to study the crush behavior of rotationally symmetric shells strengthened by circumferential ring stiffeners. The stiffner acts initially as a clamping ring until the force reaches a critical level. Then the ring becomes a rigid boss. Thus the determination of the initial-point load for a shell loaded by a rigid boss provides a basis for studying the optimum design of stiffened plastic shells against crash. In the optimum design the rigidity of the stiffeners must be compatible with the local crushing strength of the shell. This problem will be studied in detail in a future publication.

Acknowledgement

This work was supported by the Structural Mechanics Program of O.N.R. (Contract N00014-80-C-0616, Project NR 064-651). The assistance of Mr. Keating Keays in performing some of the numerical calculations is gratefully acknowledged.

References

1. Pogorielov, A.V., Bending of Convex Surfaces (in Russian), Moscow, 1951.
2. Pogorielov, A.V., Geometrical Methods in Nonlinear Theory of Elastic Shells (in Russian), Izd. Nauka, Moscow, 1967.
3. Zukasiewicz, S. and Szyszkowski, W., Geometrical Analysis of Large Elastic Deflections of Axially Compressed Cylindrical and Conical Shells, Int. J. Non-Linear Mechanics, 44, 1979, pp. 273-284.
4. Foster, C.G., Some Observations on the Yoshimura Buckle Pattern for Thin-Walled Cylinders (Part I), and Estimation of the Collapse Loads of Thin-Walled Cylinders in Axial Compression (Part II), J. Applied Mechanics, 46, 1979, pp. 377-385.
5. Pugsley, A.G. and Macaulay, M.A., The Large Scale Crumpling of Thin Cylindrical Columns, Quart. J. Mechanics Applied Mathematics, 13, 1960, pp. 1-
6. Pugsley, A.G., On the Crumpling of Thin Tubular Struts, Quart. J. Mechanics Applied Mathematics, 32, 1979, pp. 1-7.
7. Alexander, J.M., An Approximate Analysis of the Collapse of Thin Cylindrical Shells Under Axial Load, Quart. J. Mechanics Applied Mathematics, 13, 1969, pp. 10-15.
8. Johnson, W., Soden, P.D. and Al-Hassani, S.T.S., Inextensional Collapse of Thin-Walled Tubes Under Axial Compression, J. Strain Analysis, 12, 1977, pp. 317-330.
9. Pian, T.H.H., Dynamic Response of Thin Shell Structures, Proc. 2nd Symposium on Naval Structural Mechanics, Editors E.H. Lee and P.S. Symonds, Pergamon Press 1960, pp. 443-452.
10. Al-Hassani, S.T.S., Johnson, W. and Lowe, W.T. Characteristics of Inversion Tubes Under Axial Loading, J. Mechanical Engineering Sciences, 14, 1972, pp. 370-381.
11. Abramowicz, W., Mechanics of the Crushing Process of Plastic Shells, (in Polish) Ph.D. Thesis, Institute of Fundamental Technological Research, Warsaw, February 1981.
12. Updike, D.P. and Kalnins, A., Axisymmetric Behavior of an Elastic Spherical Shell Compressed Between Rigid Plates, J. Applied Mechanics, 37, 1970, pp. 635-640.

13. Updike, D.P. and Kalnins, A., Axisymmetric Postbuckling and Nonsymmetric Buckling of a Spherical Shell Compressed Between Rigid Plates, *J. Applied Mechanics*.
14. Updike, D.P., On the Large Deformation of a Rigid Plastic Spherical Shell Compressed by a Rigid Plate, *J. Engineering for Industry*, 1972, pp. 949-955.
15. Kitching, R., Houlston, R. and Johnson, W., A Theoretical and Experimental Study of Hemispherical Shells Subjected to Axial Loads Between Flat Plates, *Int. J. Mechanical Sciences*, 17, 1975, pp. 693-703.
16. Leckie, F.A. and Penny, R.K., Plastic Instability of a Spherical Shell, *Engineering Plasticity* (Ed. J. Heyman and F.A. Leckie), Cambridge University Press, 1968.
17. Morris, A.J. and Calladine, C.R., The Local Strength of a Thin Spherical Shell Loaded Radially Through a Rigid Boss, *Proc. 1st Int. Conf. on Pressure Vessel Technology*, ASEM, 1969.
18. Calladine, C.R., Simple Ideas in the Large-Deflection Plastic Theory of Plates and Slabs, *Engineering Plasticity* (Ed. J. Heyman and F.A. Leckie), Cambridge University Press, 1968.
19. Duszek, M., Plastic Analysis of Shallow Spherical Shells at Moderately Large Deflection, *Theory of Thin Shells*, IUTAM Symposium, Copenhagen, 1967, pp. 374-388.
20. Jones, N. and Ich, N.T., The Load Carrying Capacities of Symmetrically Loaded Shallow Shells, *Int. J. Solids and Structures*, 8, 1972, pp. 1339-1352.
21. Kondo, K. and Pian, T.H.H., Large Deformations of Rigid-Plastic Shallow Spherical Shells, *Int. J. Mechanical Sciences*, 23, 1981, pp. 69-76.
22. Morris, A.J. and Calladine, C.R., Simple Upper-Bound Calculations for the Indentation of Cylindrical Shells, *Int. J. Mechanical Sciences*, 13, 1971, pp. 331-343.
23. Mavrikios, Y., Oliveira, J.G. de and Wierzbicki, T., The Lateral Crushing of Long Cylindrical Shells (in preparation).
24. Hopkins, H.G., On the Plastic Theory of Plates, *Proceeding, Royal Society, London, Series A*, Vol. 241, 1957, pp. 153-179.
25. Hopkins, H.G. and Prager, W., On the Dynamic of Plastic Circular Plates, *ZAMP*, 4, 1954, pp. 317-330.

26. Jones, N., A Theoretical Study of the Dynamic Plastic Behavior of Beams and Plates with Finite-Deflections, Int. J. Solids and Structures, 7, 1971, pp. 1007-1029.
27. Stolarski, H., Assessment of Large Displacement of a Rigid-Plastic Shell Withholding a Localised Impact, Nuclear Engineering Design 41, 1977, pp. 327-334.

List of Figures

- Figure 1. Discontinuities of a function f and its derivatives at a moving hinge line.
- Figure 2. Geometry and kinematics of a rotationally symmetric shell with a moving inner and outer hinge circles.
- Figure 3. Localized zone of plastic deformation in a thin shell.
- Figure 4. Position of the axis of instantaneous rotation in thick shallow shells or in the initial phase of shell loading.
- Figure 5. Optimum values of the parameters b and ξ at various stages of the deformation process.
- Figure 6. Geometry of the tube inversion.
- Figure 7. Geometry of partially inverted conical shell.
- Figure 8. Geometry of partially crushed spherical shell.
- Figure 9. Exact and approximate force - displacement curves for a spherical shell under point load.
- Figure 10. Deformed spherical shell in the initial stage of loading.
- Figure 11. Crushing characteristics of point loaded spherical shells as predicted by various solutions.
- Figure 12. Comparison of two solutions for a spherical shell compressed between rigid plates.
- Figure 13. Effect of the width of a rigid boss on the crushing behavior of a spherical shell.
- Figure 14. A "snap-through" phenomenon in the initial stage of a rigid boss loading.
- Figure 15. Geometry of a spherical cap under external pressure loading.
- Figure 16. Initial collapse load predicted by the present solution and Ref. [21].
- Figure 17. Load versus central deflection of a spherical cap subjected to pressure loading.
- Figure 18. Effect of the boundary condition of a spherical shell on the magnitude of the crushing force.

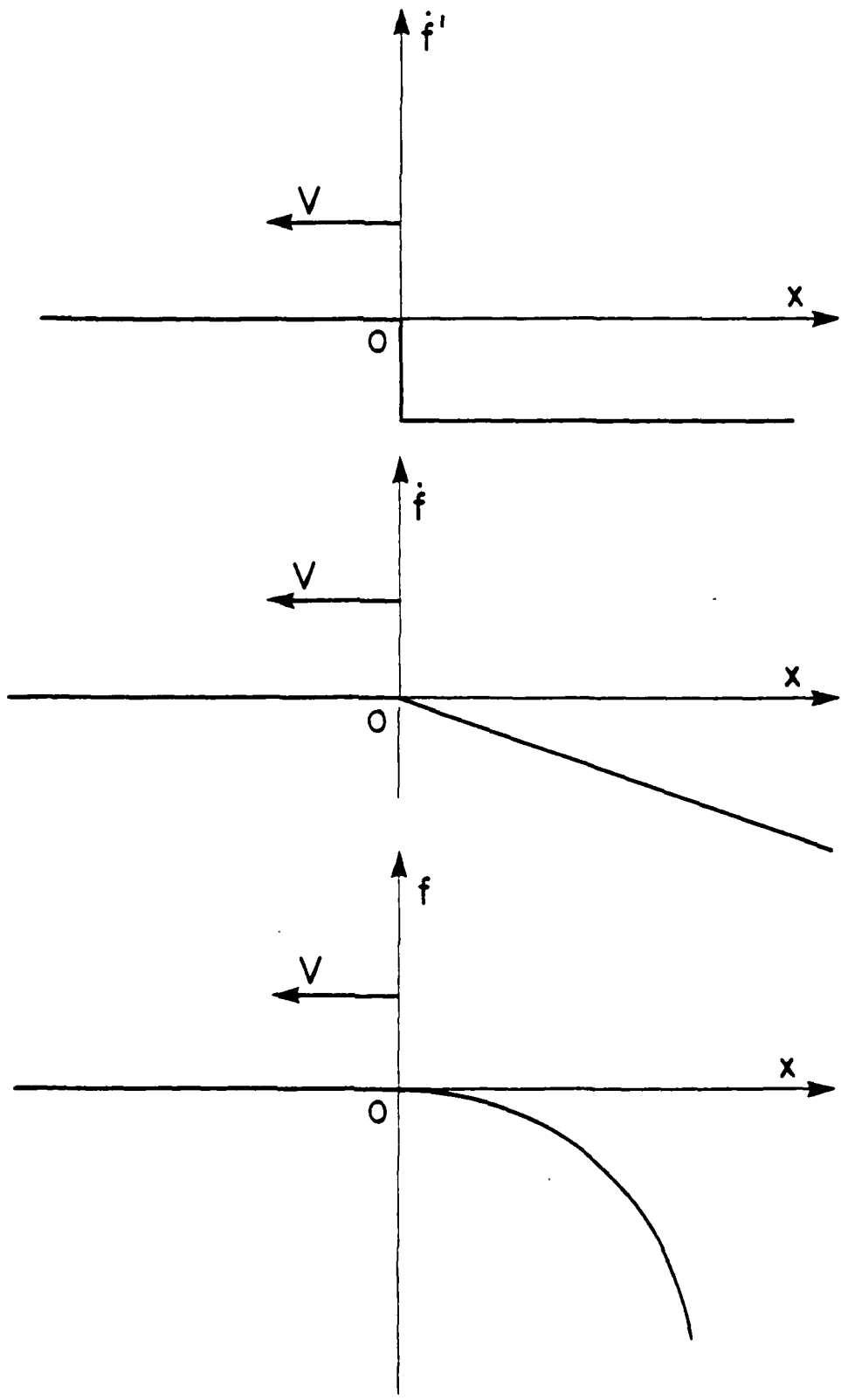


FIGURE I

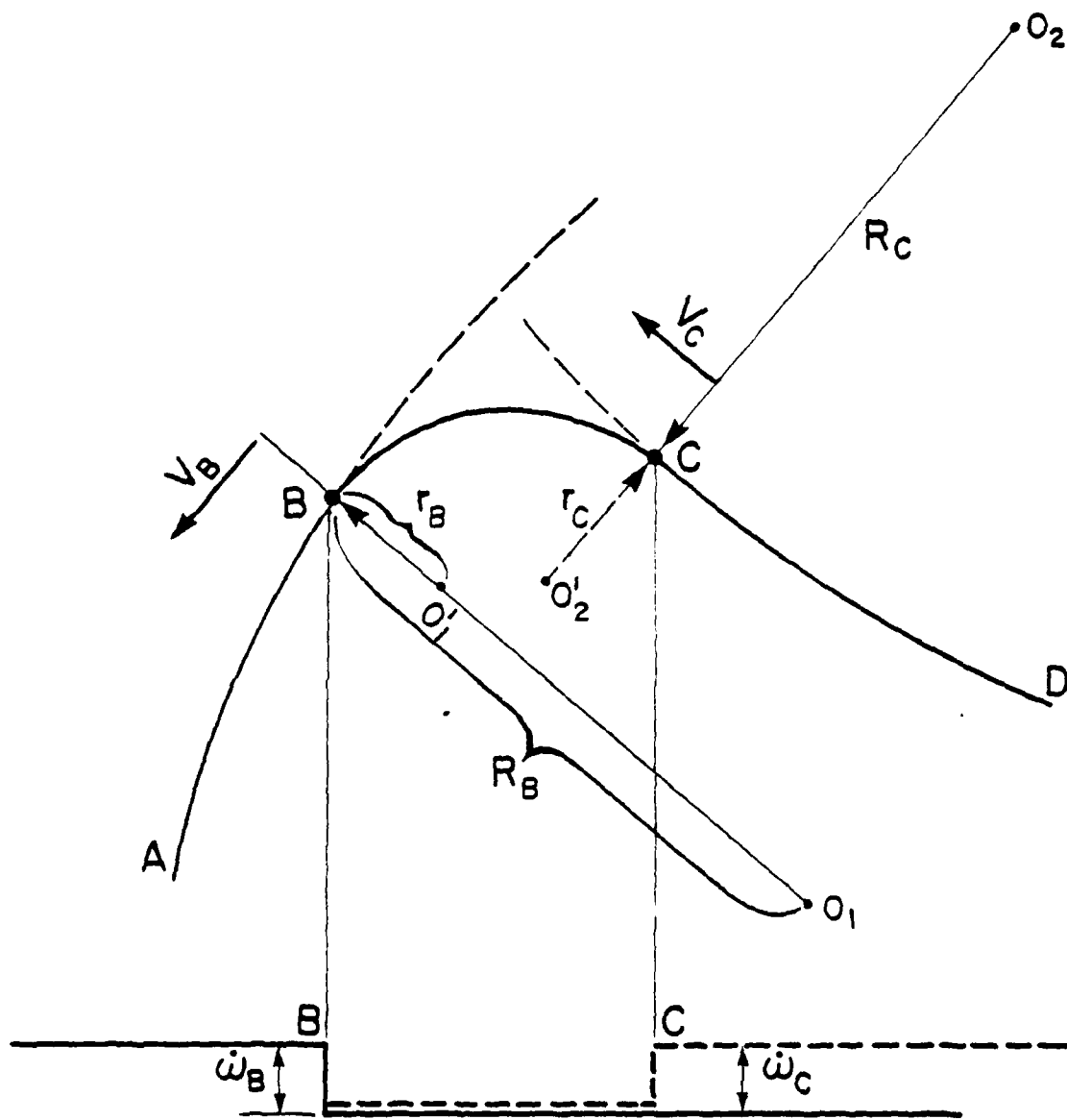


FIGURE 2

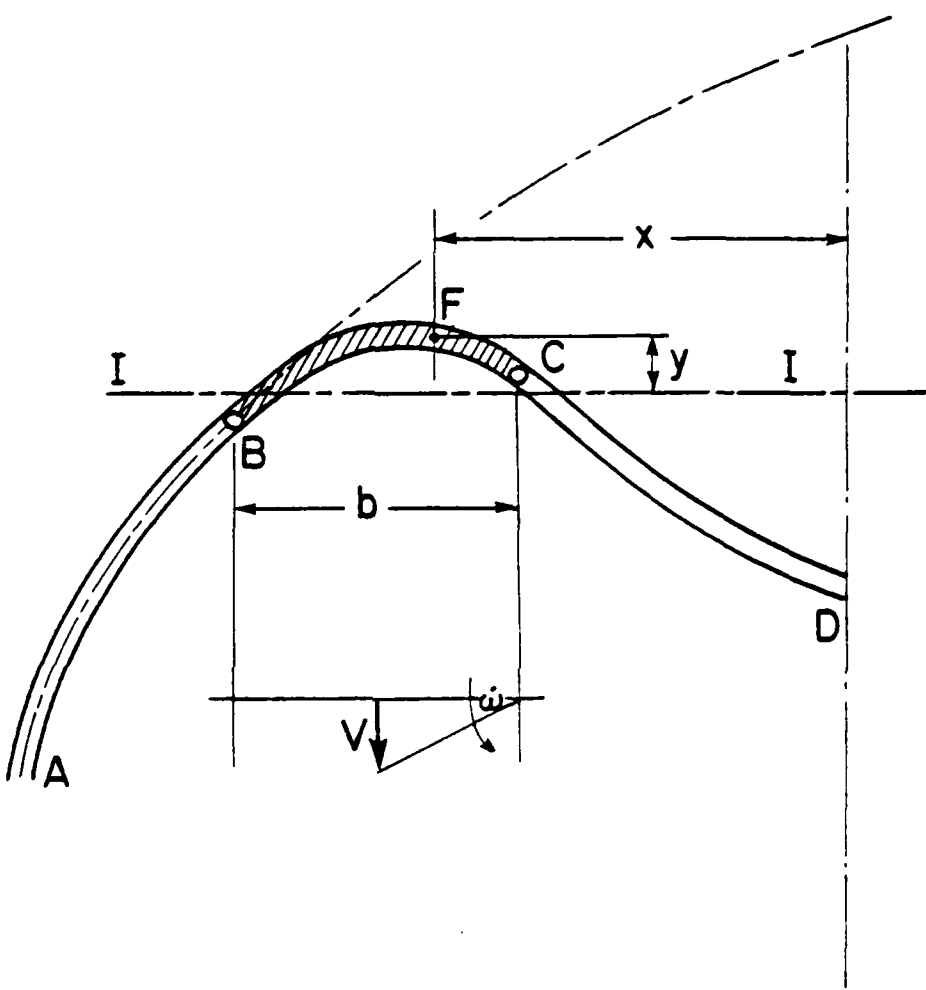


FIGURE 3

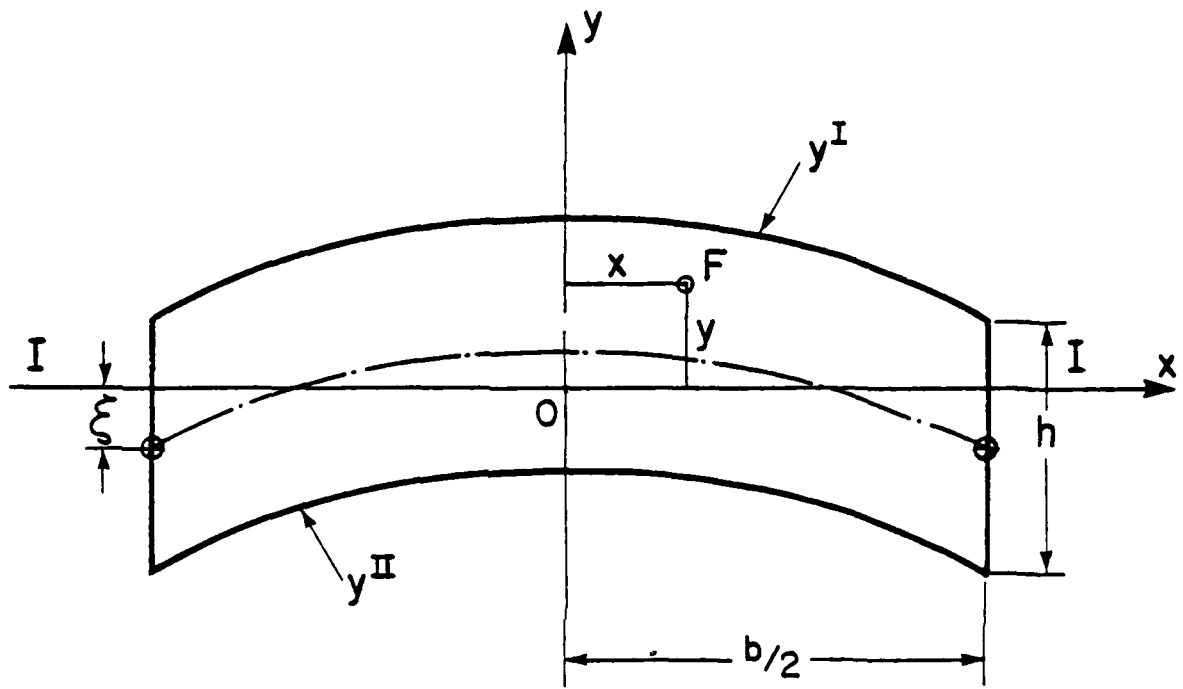


FIGURE 4

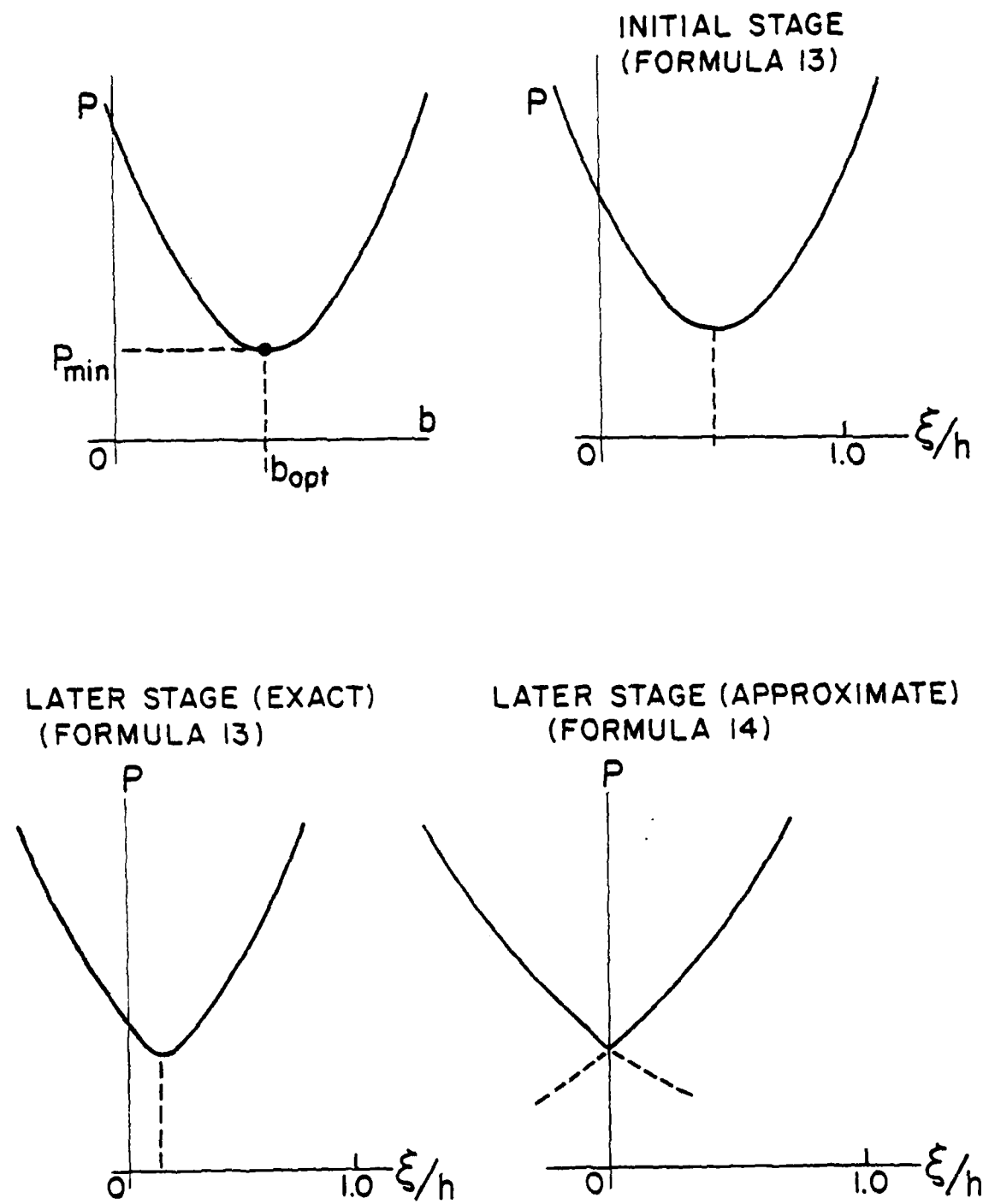


FIGURE 5

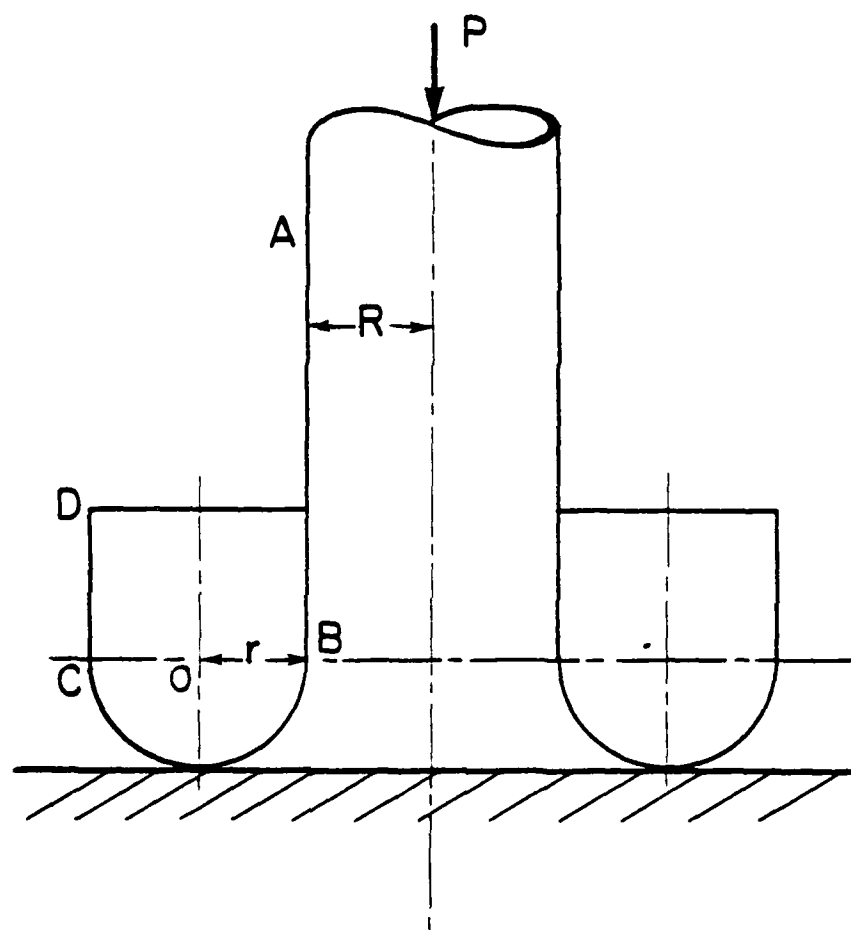


FIGURE 6

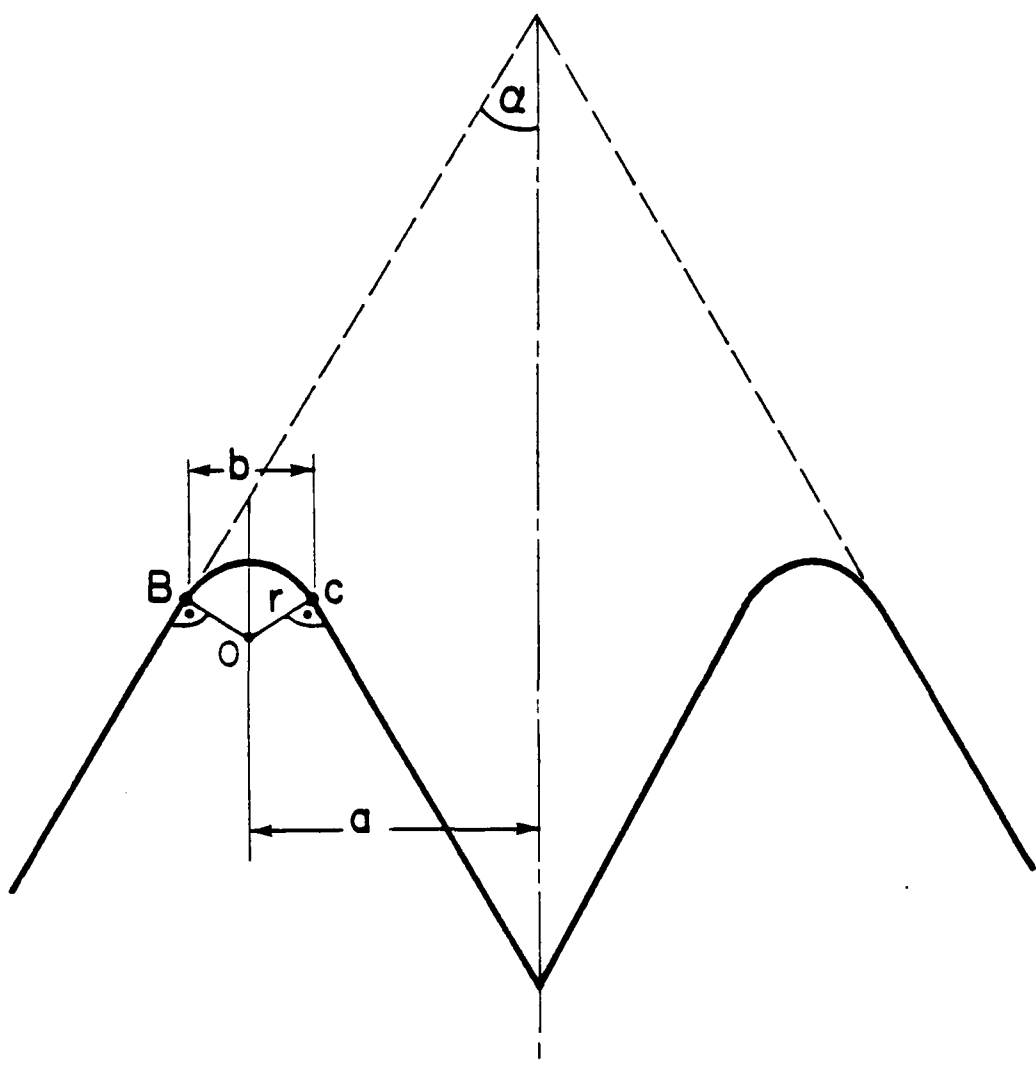


FIGURE 7

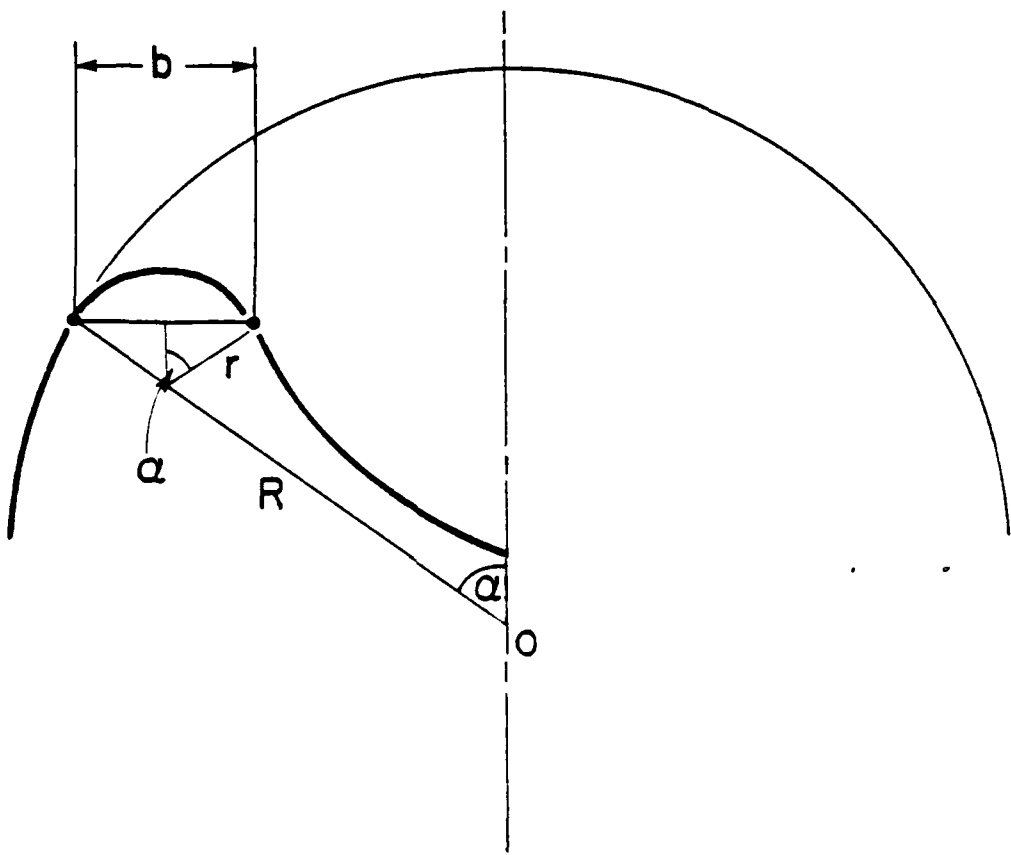


FIGURE 8

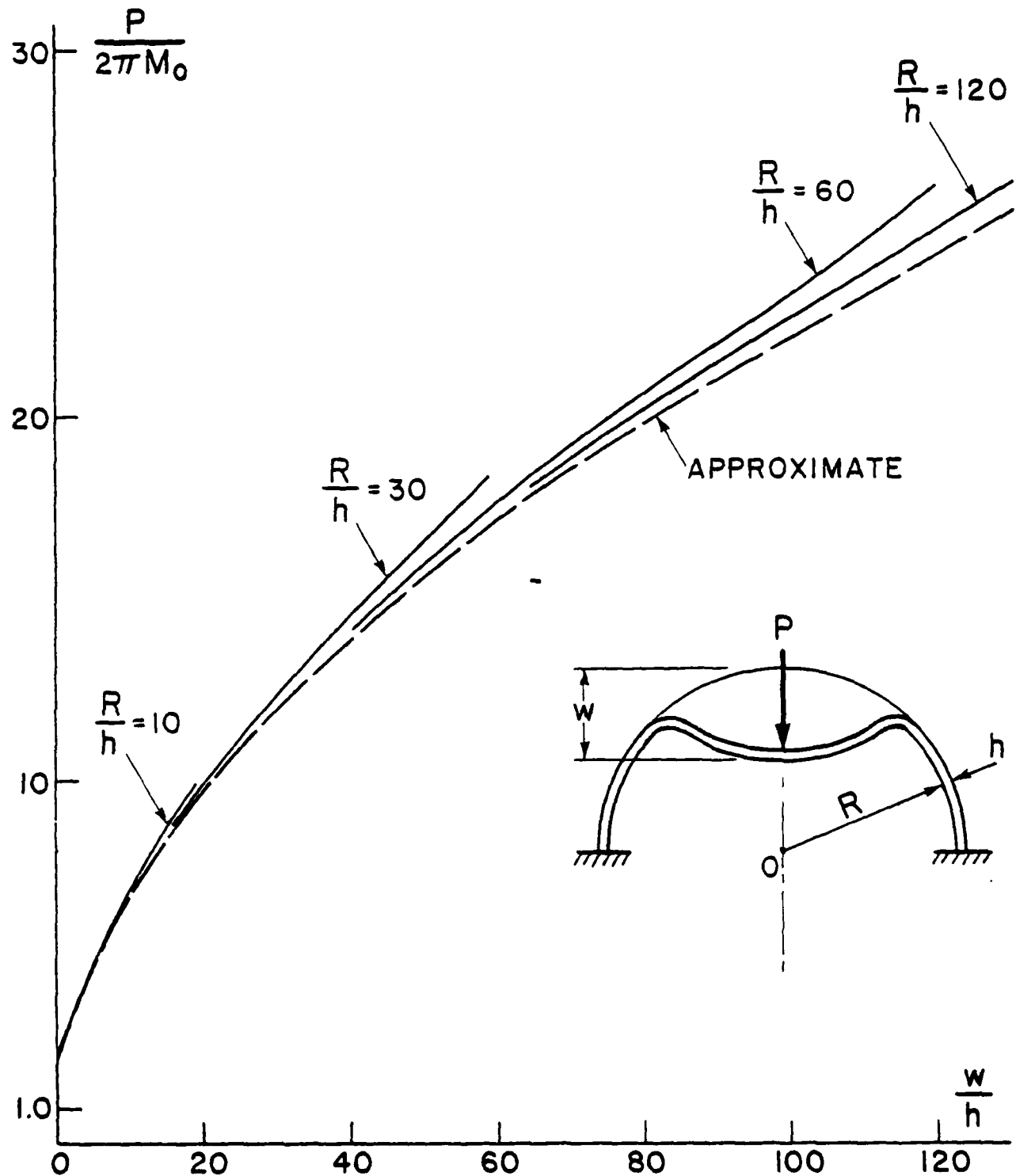


FIGURE 9

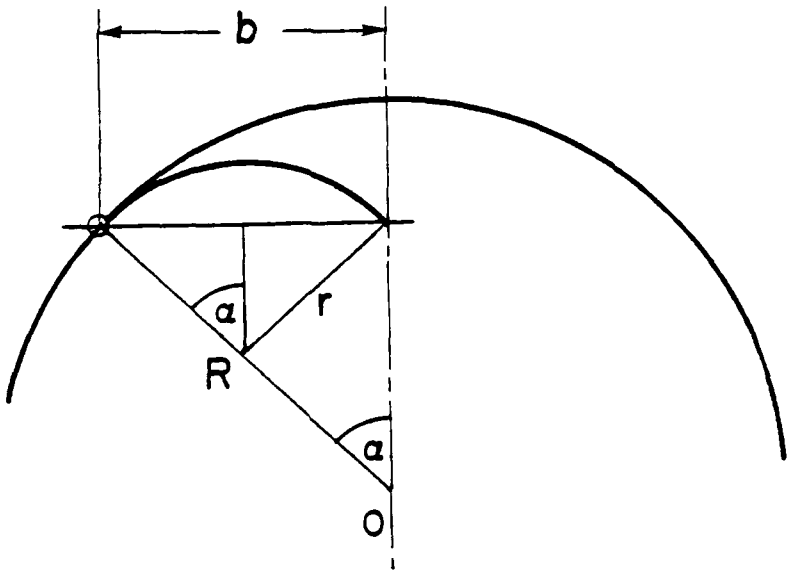


FIGURE 10

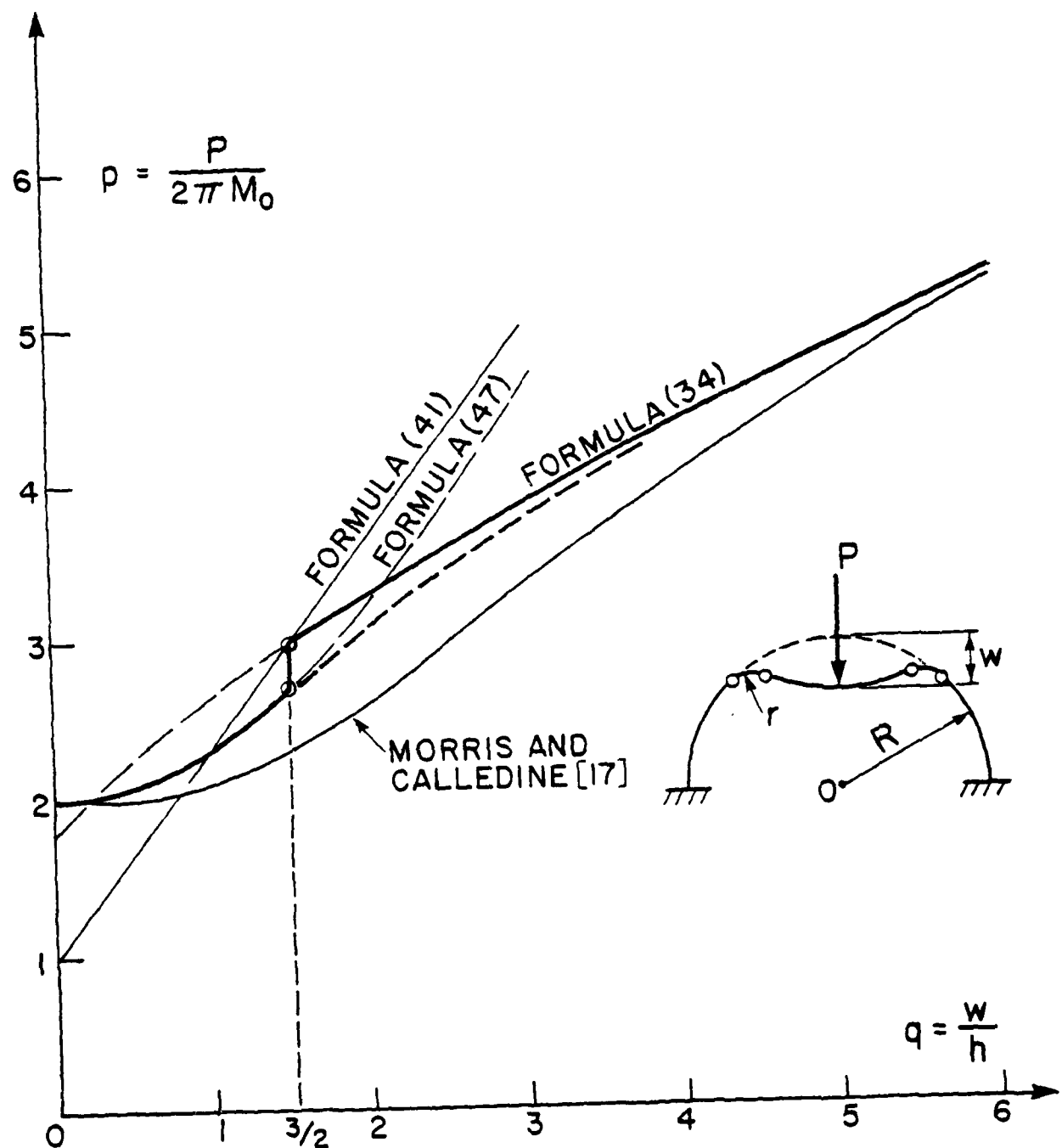


FIGURE 11

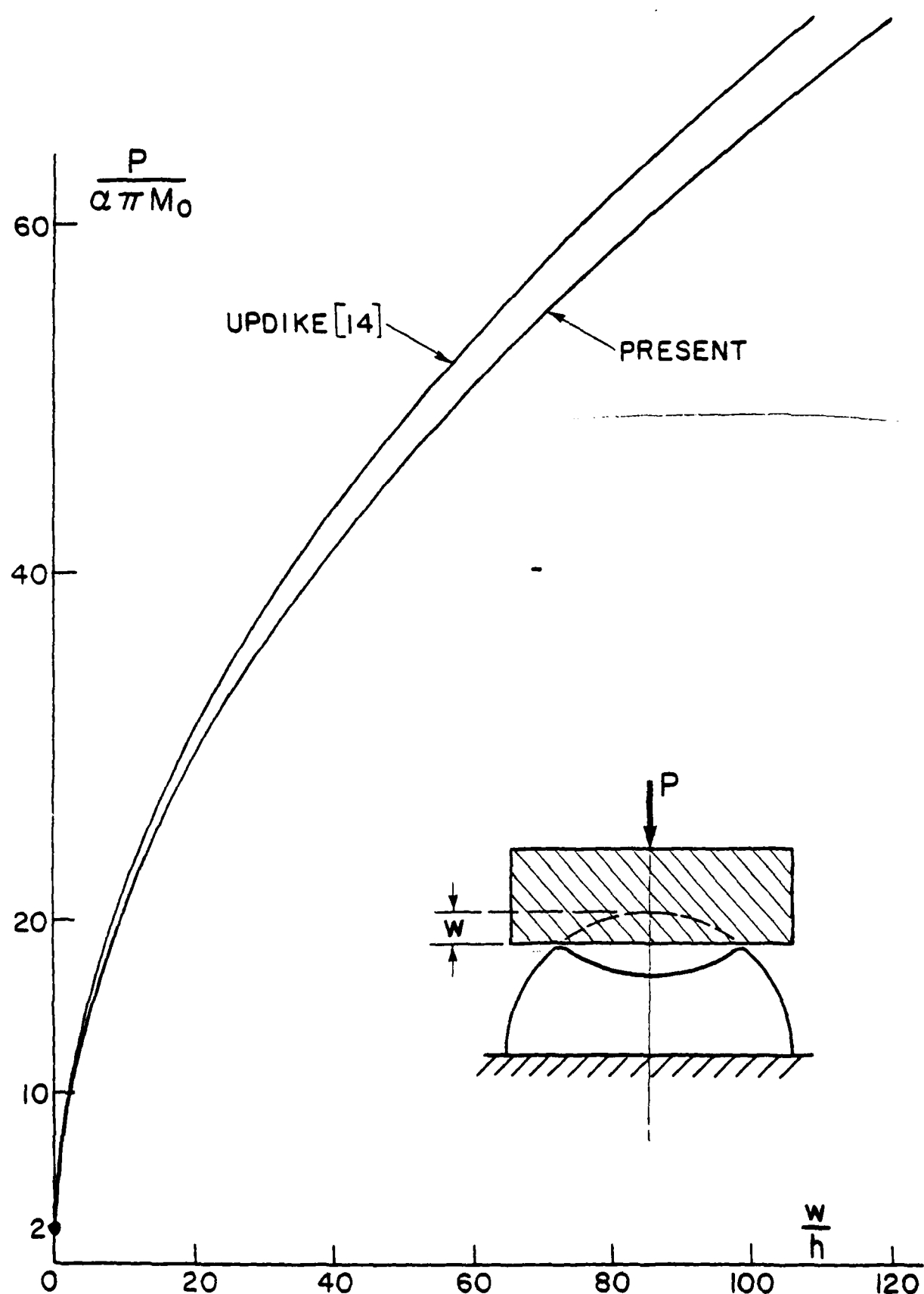


FIGURE 12

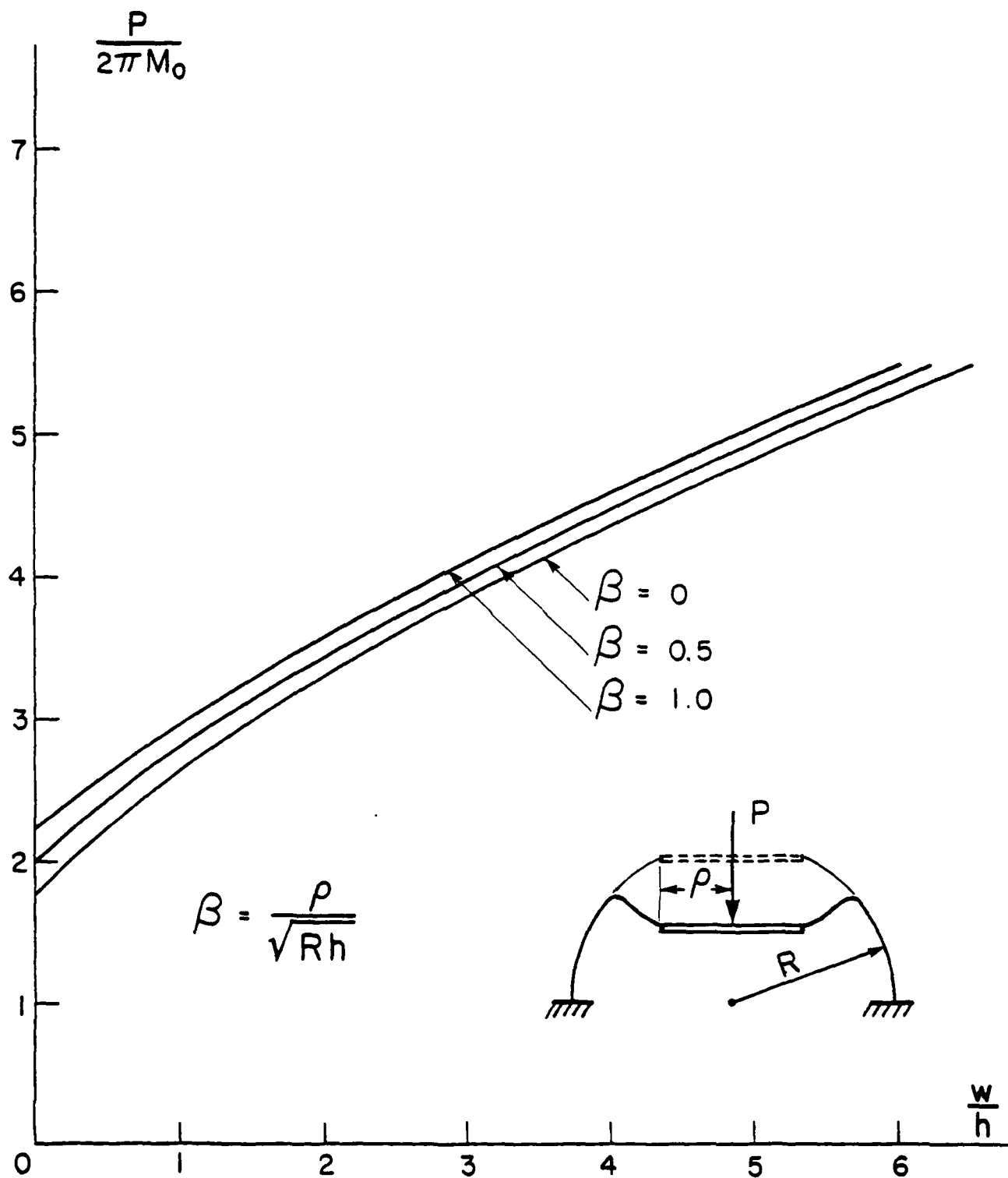


FIGURE 13

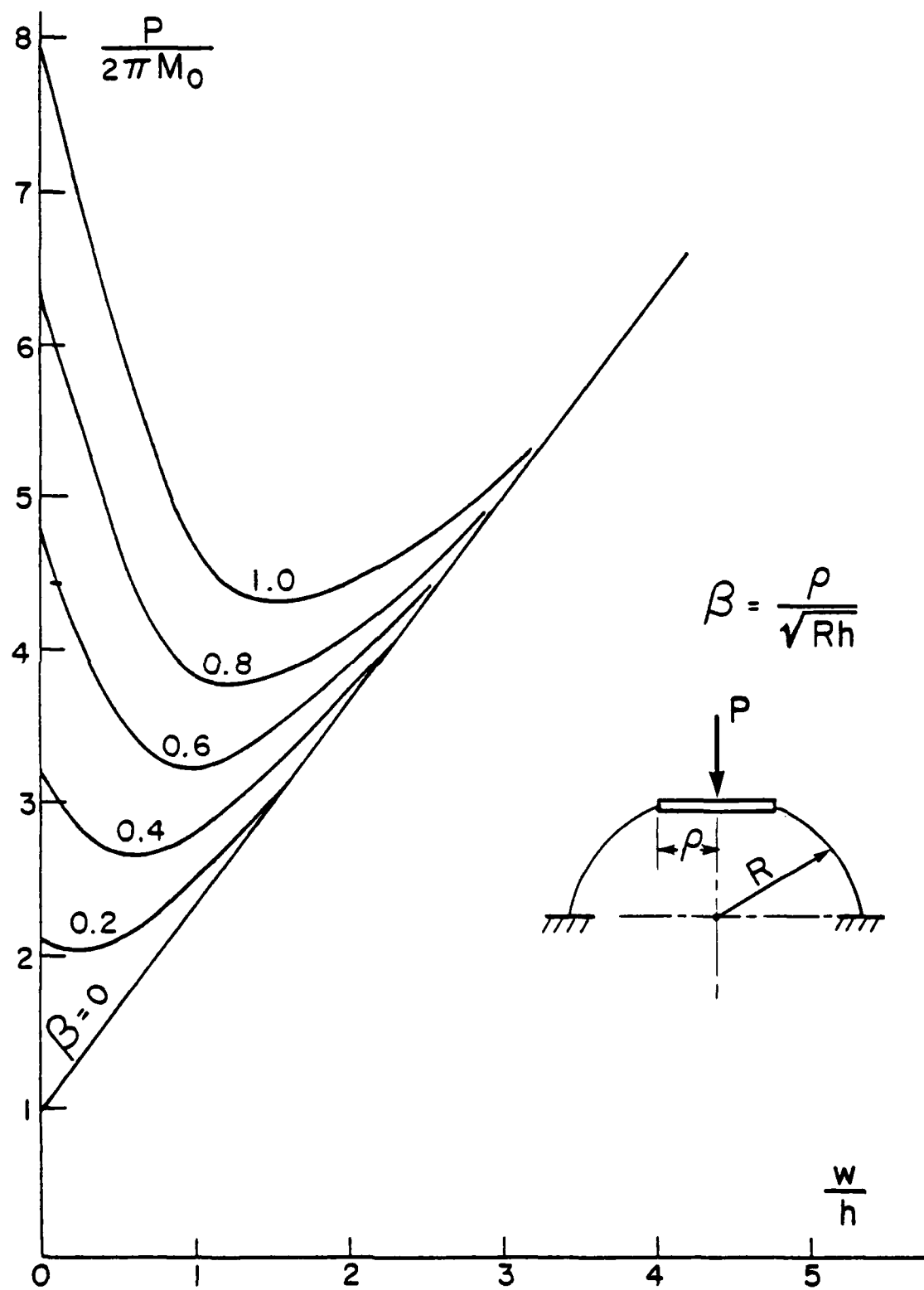


FIGURE 14

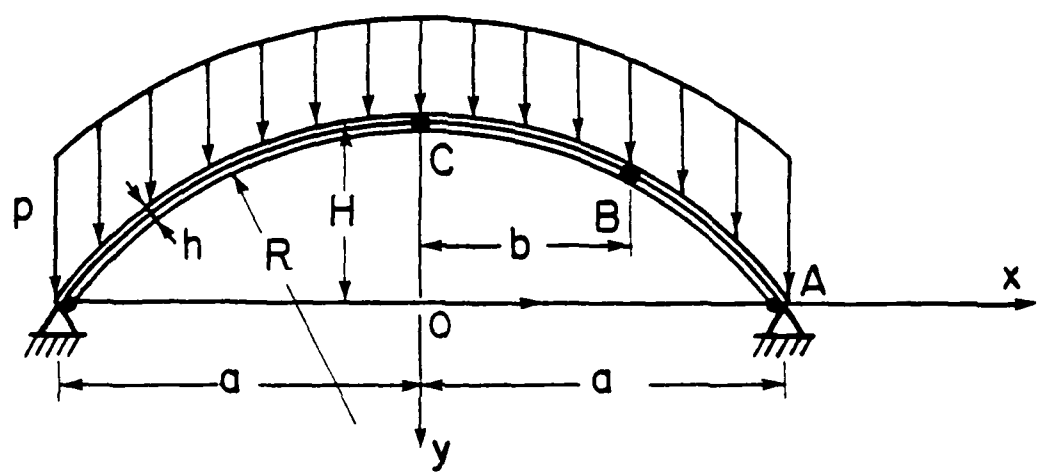


FIGURE 15

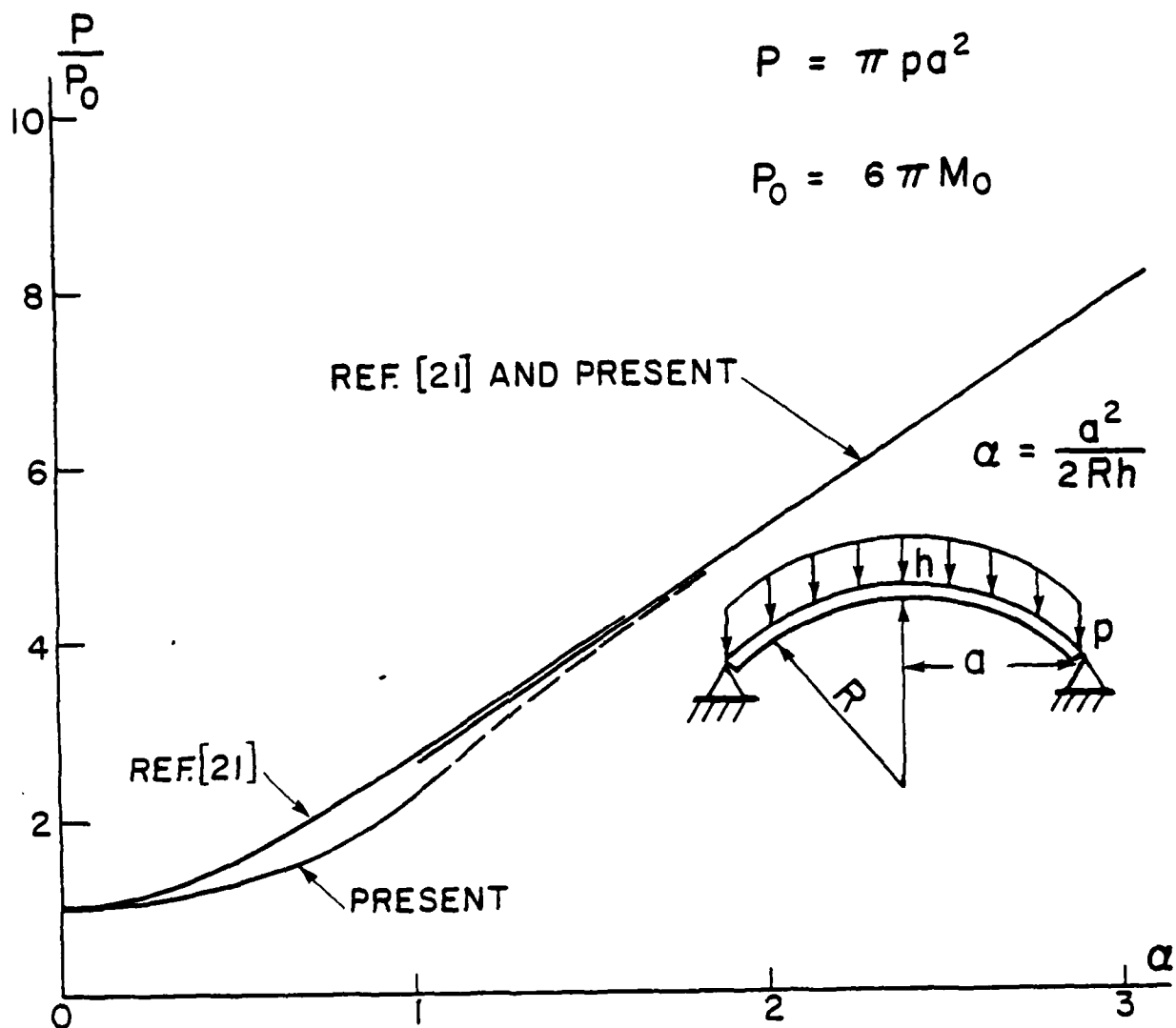


FIGURE 16

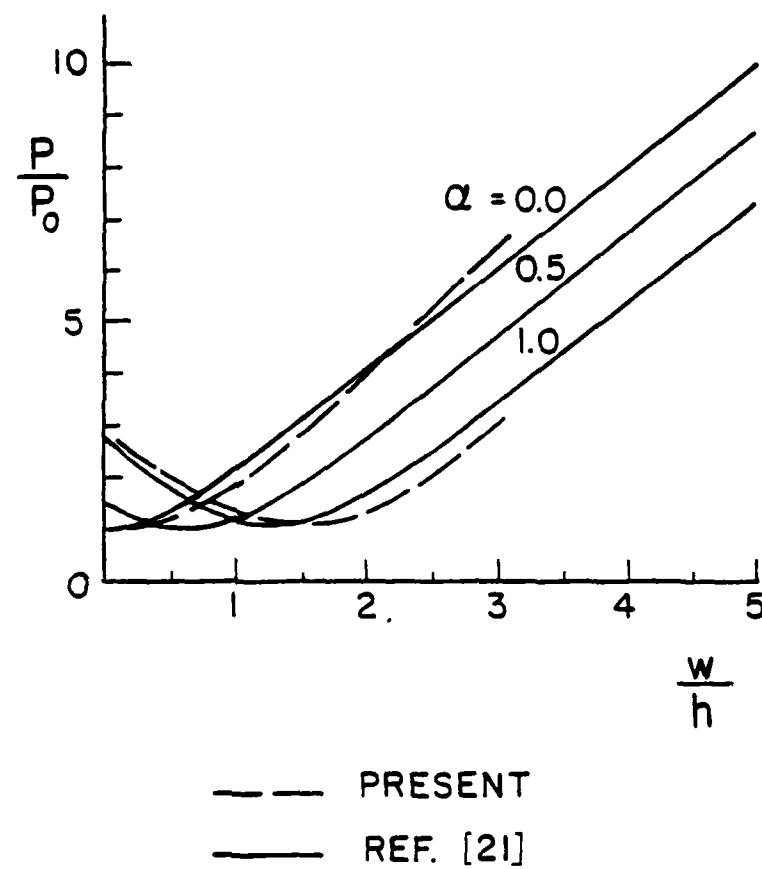


FIGURE 17

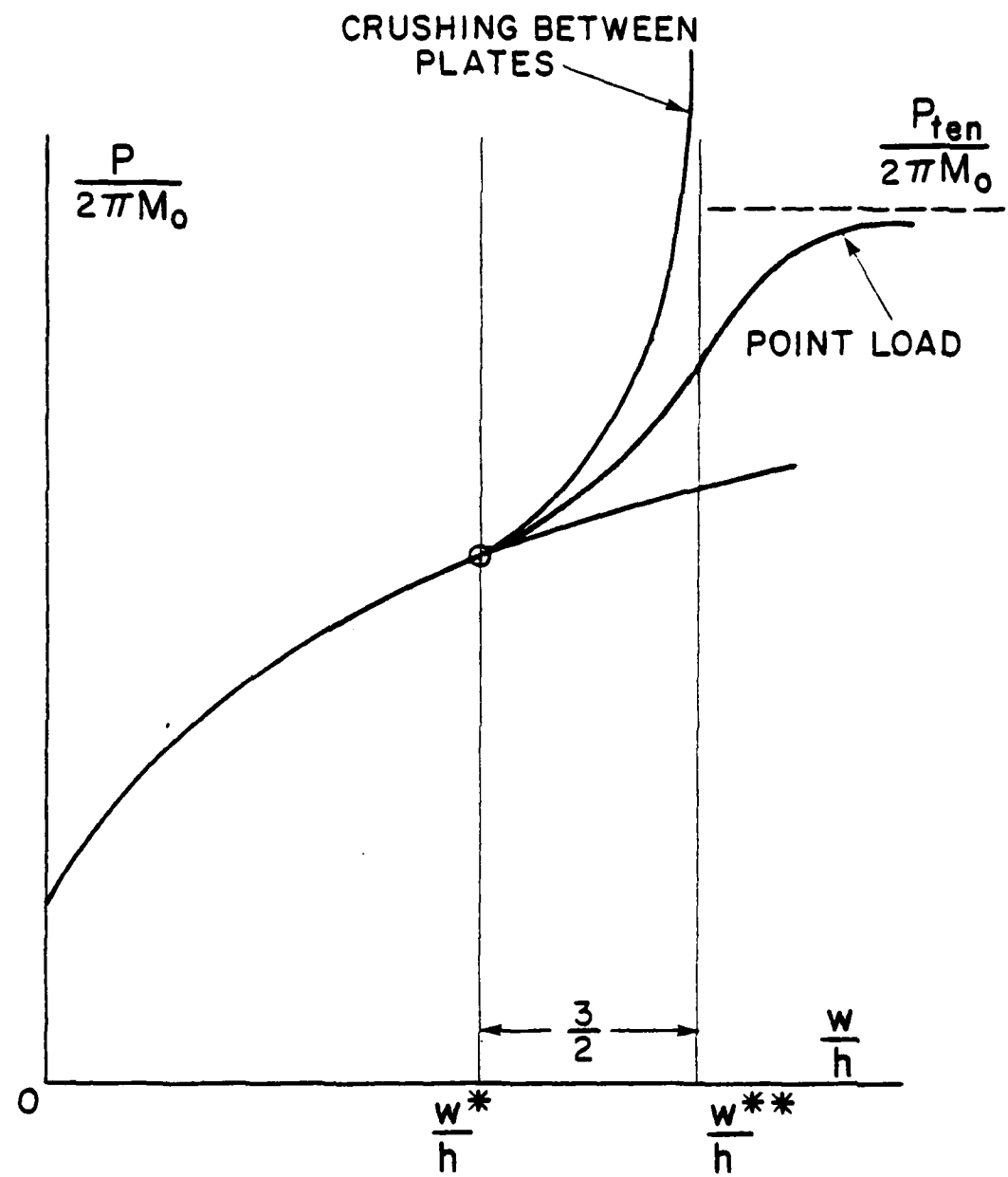


FIGURE 18

The crushing analysis of rotationally symmetric plastic shells undergoing very large deflections is presented. A general methodology is developed and simple closed form solutions which can be useful for practical applications are derived for the case of a conical shell and a spherical shell under point load, a spherical shell crushed between rigid plates and under boss loading, and a spherical cap under external uniform pressure. The effect of the end conditions and the limitations of this approach are discussed in detail.

The crushing analysis of rotationally symmetric plastic shells undergoing very large deflections is presented. A general methodology is developed and simple closed form solutions which can be useful for practical applications are derived for the case of a conical shell and a spherical shell under point load, a spherical shell crushed between rigid plates and under boss loading, and a spherical cap under external uniform pressure. The effect of the end conditions and the limitations of this approach are discussed in detail.

Plastic
Crushing
Axisymmetric
Shells

Plastic
Crushing
Axisymmetric
Shells

The crushing analysis of rotationally symmetric plastic shells undergoing very large deflections is presented. A general methodology is developed and simple closed form solutions which can be useful for practical applications are derived for the case of a conical shell and a spherical shell under point load, a spherical shell crushed between rigid plates and under boss loading, and a spherical cap under external uniform pressure. The effect of the end conditions and the limitations of this approach are discussed in detail.

Plastic
Crushing
Axisymmetric
Shells

Plastic
Crushing
Axisymmetric
Shells

The crushing analysis of rotationally symmetric plastic shells undergoing very large deflections is presented. A general methodology is developed and simple closed form solutions which can be useful for practical applications are derived for the case of a conical shell and a spherical shell under point load, a spherical shell crushed between rigid plates and under boss loading, and a spherical cap under external uniform pressure. The effect of the end conditions and the limitations of this approach are discussed in detail.

SECURITY CLASSIFICATION OF THIS PAGE (When Data Entered)

REPORT DOCUMENTATION PAGE			READ INSTRUCTIONS BEFORE COMPLETING FORM
1. REPORT NUMBER Ocean Engineering Report 81-8	2. GOVT ACCESSION NO. <i>HD-A 102 999</i>	3. RECIPIENT'S CATALOG NUMBER	
4. TITLE (and Subtitle) CRUSHING ANALYSIS OF ROTATIONALLY SYMMETRIC PLASTIC SHELLS	5. TYPE OF REPORT & PERIOD COVERED Technical Report		
	6. PERFORMING ORG. REPORT NUMBER 81-8		
7. AUTHOR(s) Joao G. de Oliveira Tomasz Wierzbicki	8. CONTRACT OR GRANT NUMBER(s) N00014-80-C-0616		
9. PERFORMING ORGANIZATION NAME AND ADDRESS Department of Ocean Engineering Massachusetts Institute of Technology Cambridge, Massachusetts 02139	10. PROGRAM ELEMENT, PROJECT, TASK AREA & WORK UNIT NUMBERS NR 064-651		
11. CONTROLLING OFFICE NAME AND ADDRESS ONR Code 474 Arlington, VA 22217	12. REPORT DATE 6/30/81		
14. MONITORING AGENCY NAME & ADDRESS (if different from Controlling Office)	13. NUMBER OF PAGES 64		
	15. SECURITY CLASS. (of this report) Unclassified		
	15a. DECLASSIFICATION/DOWNGRADING SCHEDULE		
16. DISTRIBUTION STATEMENT (of this Report) This document has been approved for public release and sale; distribution is unlimited.			
17. DISTRIBUTION STATEMENT (of the abstract entered in Block 20, if different from Report)			
18. SUPPLEMENTARY NOTES			
19. KEY WORDS (Continue on reverse side if necessary and identify by block number) Plastic Crushing, Axisymmetric Shells			
20. ABSTRACT (Continue on reverse side if necessary and identify by block number) The crushing analysis of rotationally symmetric plastic shells undergoing very large deflections is presented. A general methodology is developed and simple closed form solutions which can be useful for practical applications are derived for the case of a conical shell and a spherical shell under point load, a spherical shell crushed between rigid plates and under boss loading, and a spherical cap under external uniform pressure. The effect of the end conditions and the limitations of this approach are discussed			

Unclassified

-61-

SECURITY CLASSIFICATION OF THIS PAGE(When Data Entered)

in detail.

Unclassified

SECURITY CLASSIFICATION OF THIS PAGE(When Data Entered)